Copy 165

[redacted]

NASA TM X-744

NASA TM X-744

[redacted]

TECHNICAL MEMORANDUM

Declassified by authority of NASA
Classification Change Notices No. 113 X-744
Dated ** 6/28/67

DECLASSIFIED-AUTHORITY-MEMO.US:
2313. TAINE TO SHAUKLAS
DATED JUNE 15, 1967

LOW-SPEED LONGITUDINAL STABILITY CHARACTERISTICS OF A SUPERSONIC TRANSPORT CONFIGURATION WITH VARIABLE-SWEEP WINGS EMPLOYING A DOUBLE INBOARD PIVOT

By William P. Henderson

Langley Research Center
Langley Station, Hampton, Va.

[redacted]

ADVANCE COPY

FACILITY FORM 602

(ACCESSION NUMBER)	(THRU)
52	1
(PAGES)	(CODE)
TMX-744	02
(NASA CR OR TMX OR AD NUMBER)	(CATEGORY)

CLAS[redacted]

This material contains [redacted] person is prohibited by law.

NATIONAL AERONAUTICS AND SPACE ADMINISTRATION
WASHINGTON

[redacted]

DECL[redacted]IFIED

NATIONAL AERONAUTICS AND SPACE ADMINISTRATION

TECHNICAL MEMORANDUM X-744

LOW-SPEED LONGITUDINAL STABILITY CHARACTERISTICS OF A SUPERSONIC TRANSPORT CONFIGURATION WITH VARIABLE-SWEEP WINGS EMPLOYING A DOUBLE INBOARD PIVOT*

By William P. Henderson

Declassified by authority of NASA
Classification Change Notices No. 113
Dated ** 6/28/67

ABSTRACT

The investigation was made in the Langley high-speed 7- by 10-foot tunnel. Tests were made at a dynamic pressure of 100 pounds per square foot and at angles of attack from -2° to 24°. The test Reynolds number, based on the mean aerodynamic chord, was 2.04×10^6. The effects of canard, horizontal tails, wing sweep, and engine arrangements on the longitudinal aerodynamic characteristics are presented. The effect of adding fixed area (fore wings) to the 35° sweptback wing is also presented.

*Title, Unclassified.

L-3053

[redacted]

[redacted]

NATIONAL AERONAUTICS AND SPACE ADMINISTRATION

TECHNICAL MEMORANDUM X-744

LOW-SPEED LONGITUDINAL STABILITY CHARACTERISTICS OF A SUPERSONIC TRANSPORT CONFIGURATION WITH VARIABLE-SWEEP WINGS EMPLOYING A DOUBLE INBOARD PIVOT*

By William P. Henderson

SUMMARY

An investigation was made in the Langley high-speed 7- by 10-foot tunnel to determine the effect of a double-inboard-pivot variable-sweep wing on the low-speed longitudinal stability characteristics of a supersonic commercial air transport (SCAT 12-B) configuration. Tests were made at a Mach number of 0.267 and at angles of attack from -2° to 24°. The test Reynolds number, based on the mean aerodynamic chord, is 2.04×10^{6}.

The results indicate that there is essentially no change in the stability level of the 35° and 75° sweptback-wing positions. The change between the stability level of the 35° sweptback wing at a Mach number of 0.267 and that of the 75° sweptback wing at a Mach number of 2.86 is 7.9 percent of the mean aerodynamic chord. The static margin is 6.5 percent of the mean aerodynamic chord less when the fore wing is retracted into the fuselage than when the fore wing remains in the extended position, as the main wing is swept forward from the 75° to the 35° sweptback positions. The addition of a chord extension to the main-wing panel of the configuration with the wing in the 35° sweptback position leads to acceptable pitching-moment variations with angle of attack.

INTRODUCTION

The National Aeronautics and Space Administration is studying the aerodynamic characteristics of configurations that may be suitable for supersonic transport designs. (For example, see refs. 1 to 9.) It has been shown that reasonable range capabilities can be obtained in the supersonic cruise condition by a configuration utilizing a highly swept or thin low-aspect-ratio wing (refs. 4 and 6). However, these types of configuration have geometrical characteristics that are not compatible with those needed for efficient subsonic flight characteristics. In order to obtain a configuration that has efficient aerodynamic characteristics throughout the flight regime, some method of varying the geometry of the wing is required. One such method of obtaining variable geometry is to provide a configuration whose wing leading-edge sweep angle may be varied in flight. This

*Title, Unclassified.

[redacted]

method would provide the configuration with a high-aspect-ratio low-sweep wing for the subsonic portion of the flight and a low-aspect-ratio highly swept wing for the supersonic portion of the flight.

One of the major aerodynamic problems associated with variable-sweep wings is that of reducing the variation of longitudinal stability with wing sweep. One solution is the use of an outboard pivot location (refs. 10 and 11) which, if properly chosen, can essentially eliminate the aerodynamic-center shift. Another type of pivot arrangement utilized on the wing of an attack-airplane configuration has been tested at subsonic and supersonic speeds, and the results are presented in reference 12. This wing and pivot arrangement is referred to as a double-inboard-pivot variable-sweep wing. For this type of wing, two pivot mechanisms located within the fuselage are utilized for each wing panel. One pivot is for the main wing and the second is for an extendible fore wing. The purpose of this type of arrangement is to take advantage of the fuselage depth for housing the pivot (from structural considerations) while still reducing the variation of aerodynamic center with wing-sweep angle, and to avoid the discontinuous (or broken) wing leading edges at designated sweep angles. The aerodynamic-center shift for this type of configuration is controlled by having the fore wing housed in the fuselage when the main wing is in its low-sweep position and, as the main wing is swept backward, the fore wing is extended outward becoming the forward portion of the wing.

The purpose of this paper, in view of the favorable results obtained on the attack-airplane configuration of reference 12, is to present the effect of a double-inboard-pivot variable-sweep wing on the stability characteristics of a transport configuration. This investigation was made in the Langley high-speed 7- by 10-foot tunnel at a Mach number of 0.267. The investigation of this configuration has been extended to supersonic speeds and the results are presented in reference 13.

SYMBOLS

The forces and moments measured on the configuration are presented about the wind-axis system. The positive direction of the force and moments is shown in figure 1. All coefficients are based on the geometric characteristics associated with the maximum sweep condition. The center of gravity is located at 60.40 percent of the body length, as shown in figure 2.

C_L lift coefficient, $\frac{\text{Lift}}{qS_{ref}}$

C_D drag coefficient, $\frac{\text{Drag}}{qS_{ref}}$

C_m pitching-moment coefficient, $\frac{\text{Pitching moment}}{qS_{ref}}$

M Mach number

DEC[redacted]IFIED

q	dynamic pressure, lb/sq ft
S_{ref}	wing reference area, 1.285 sq ft
S_{fw}	area of fore wing
$\bar{c}$	mean aerodynamic chord, 1.149 ft
c	local wing chord, ft
b	wing span, ft
α	angle of attack, measured from fuselage reference line, deg
Λ	main-wing leading-edge sweep angle, deg
i_t	horizontal-tail incidence angle (positive nose up), deg
Γ_t	horizontal-tail anhedral angle (positive tip down), deg
δ_c	canard deflection angle (positive nose up), deg
C_{L_α}	lift-curve slope, per deg
$C_{D,min}$	minimum drag coefficient
$\frac{C_m}{C_L}$	static margin, percent $\bar{c}$
$(L/D)_{max}$	maximum lift-drag ratio

Model components:

C	canard
E	engine pack
F	fuselage
H	horizontal-tail surface
N	nacelles
V	vertical-tail surface
W	wing

Drawings of configurations tested are shown in figure 2. Two types of engine arrangements were tested on this configuration. The first was an engine pack mounted under and at the rear of the fuselage, as shown in figure 2(a). This engine pack had no provision for airflow through it. The second engine arrangement consisted of four nacelles, two mounted on the vertical tail and two mounted from pylons under the fuselage, as shown in figure 2(b). Details of the engine pack and nacelles are shown in figure 2(c).

Dimensions of the basic model components and those for the wing at sweep angles of 75°, 60°, 45°, and 35° are given in table I. The wing utilized in this configuration has two pivot locations for each wing panel, one for the main wing and the second for the extendible fore wing. When the main wing is in its maximum sweep position, the fore wing is extended outward to its maximum position. Then as the main wing is swept forward, the fore wing is retracted into the fuselage. The pivot for the main wing is located at approximately 58.2 percent of the body length and 15.7 percent of the wing semispan in the 75° sweepback position. The wing employs an NACA 65_1A012 airfoil section normal to the leading edge at the wing root and an NACA 63A009 airfoil section normal to the leading edge at the wing tip.

The canard is a 1/16-inch flat plate with beveled leading and trailing edges. The horizontal and vertical tails are identical in planform and employ an NACA 65A002 airfoil section in the streamwise direction. The vertical position of the horizontal tails is 0.4 inch ($0.029\bar{c}$) below the fuselage reference line when the nacelles are used. When the engine pack arrangement is used, the horizontal tails are mounted on the sides of the engine pack 2.63 inches ($0.191\bar{c}$) below the fuselage reference line.

The chord extension shown in figure 2(a) extended from 0.53b/2 of the main-wing panel of the configuration with the wing in the 35° sweptback position to the wing tip, had a chord of 0.090c at 0.53b/2 and 0.128c at the wing tip, and was deflected 25° in a nose-down direction.

A few wind-tunnel tests were made to determine the effect of fore-wing area added to the 35° sweptback wing. These fore wings had an area of 21.0 and 31.4 percent of the reference area. Details of the fore wings are shown in figure 3.

TESTS AND CORRECTIONS

The investigation was made in the Langley high-speed 7- by 10-foot tunnel at a Mach number of 0.267, which corresponds to a dynamic pressure of 100 pounds per square foot and a Reynolds number, based on $\bar{c}$ of the 75° sweptback wing, of 2.04×10^6.

Lift, drag, and pitching moment were measured through an angle-of-attack range of -2° to 24°.. Transition strips, 1/8 inch wide, of No. 100 carborundum

grit were placed along the 5-percent-chord line of the wing and tail surfaces and at 5 percent of the fuselage length of all configurations except the configurations for which the area of the fore wing was varied.

The angle of attack was corrected for deflection of the sting-support system under load. The drag data were corrected to correspond to a pressure at the base of the fuselage equal to the free-stream static pressure. Jet-boundary and blockage corrections were considered negligible. A drag coefficient of 0.0021 was subtracted from the data of the configuration with the four nacelles. This drag coefficient corresponds to the theoretical internal skin-friction drag of the four nacelles.

PRESENTATION OF DATA

The basic data are presented in figures 4 to 15 and some of the more pertinent results are compared and summarized in figures 16 to 24. As an aid in locating a particular portion of the data, the following outline of the content of the data figures is presented:

	Figure
Effect of wing leading-edge sweep angle on longitudinal aerodynamic characteristics of following configurations:	
WFVHCE; $\delta_c = 0^\circ$; $i_t = 0^\circ$; $\Gamma_t = 0^\circ$	4
WFVH; $i_t = 0^\circ$; $\Gamma_t = 0^\circ$	5
WFVHC; $\delta_c = 0^\circ$; $i_t = 0^\circ$; $\Gamma_t = 0^\circ$	6
WFVCE; $\delta_c = 0^\circ$	7
WFVHCN; $\delta_c = 0^\circ$; $i_t = 0^\circ$; $\Gamma_t = 0^\circ$	8
Effect of horizontal-tail incidence on longitudinal aerodynamic characteristics of WFVHCE configuration for -	
$\Lambda = 35^\circ$	9
$\Lambda = 75^\circ$	10
Effect of canard deflection on longitudinal aerodynamic characteristics of WFVHCE configuration ($i_t = 0^\circ$; $\Gamma_t = 0^\circ$) for -	
$\Lambda = 35^\circ$	11
$\Lambda = 75^\circ$	12
Effect of wing leading-edge sweep angle on longitudinal aerodynamic characteristics of WFVHCE configuration with chord extension on main wing. $\delta_c = 0^\circ$; $i_t = 0^\circ$; $\Gamma_t = 0^\circ$	13
Effect of wing leading-edge sweep angle on longitudinal aerodynamic characteristics of WFVHCE configuration with horizontal tail set at $\Gamma_t = 10^\circ$. $\delta_c = 0^\circ$; $i_t = 0^\circ$	14
Effect of wing leading-edge sweep angle on longitudinal aerodynamic characteristics of WFVHCE configuration with chord extension on main wing and horizontal tail set at $\Gamma_t = 10^\circ$. $\delta_c = 0^\circ$; $i_t = 0^\circ$	15

Figure

Effects of engine pack, tail anhedral, and chord extension on pitching-moment characteristics of WFVHC configuration ($i_t = 0^\circ$; $\delta_c = 0^\circ$) for -

$\Lambda = 35^\circ$ 16

$\Lambda = 75^\circ$ 17

Summary of longitudinal aerodynamic characteristics of WFVH configuration with and without canard. $i_t = 0^\circ$ 18

Summary of longitudinal aerodynamic characteristics of WFVCE configuration with and without horizontal tail. $\delta_c = 0^\circ$ 19

Comparison of engine arrangements on longitudinal aerodynamic characteristics of WFVHC configuration. $\delta_c = 0^\circ$; $i_t = 0^\circ$ 20

Effect of addition of fore wings on longitudinal aerodynamic characteristics of WF configuration with 35° sweptback wing 21

Effect of addition of fore wings on pitching-moment characteristics of WF configuration with 35° sweptback wing. All configurations transferred to same stability level 22

Summary of effect of fore wings on longitudinal aerodynamic characteristics of WF configuration with 35° sweptback wing 23

Effect of fore wings on longitudinal-stability variation with wing sweep for WFVH configuration 24

DISCUSSION

A comparison of the effect of various modifications made to the complete configuration on the pitching-moment variation with angle of attack and lift coefficient is shown for the 35° sweptback wing in figure 16. These data show that a rather severe instability occurs at low to moderate angles of attack for the configuration with the engine pack off and the canard and horizontal tail on. The addition of the engine pack, which allowed the horizontal tail to be lowered to a position $0.191\bar{c}$ below the fuselage reference line, had only a slight effect on the pitching-moment variation with angle of attack. By setting the horizontal tail at an anhedral angle of 10°, the pitching-moment variation with angle of attack was somewhat more linear although the instability was not eliminated. The addition of the chord extension to the main-wing panel, however, led to acceptable pitching-moment variations with angle of attack regardless of the horizontal-tail anhedral angle. A comparison of the effect of these modifications on the pitching-moment variation with angle of attack for the configuration in the 75° sweepback position is shown in figure 17. These data indicate that none of the aforementioned modifications led to satisfactory pitching-moment variation with angle of attack. However, it is believed that with slight modifications the pitching-moment variation with angle of attack could be made acceptable for an emergency landing condition when the angle of sweep cannot be decreased because of a malfunction.

A summary of the longitudinal aerodynamic characteristics of the configuration with and without the canard is shown in figure 18. These data indicate that, for the configuration without the canard, the 75° sweptback wing is 5.2 percent $\bar{c}$

more stable than the 35° sweptback wing. However, by the addition of the canard, this difference between the stability level of the 35° sweptback wing can essentially be eliminated. Thus, because of this desirable effect of there being essentially no stability difference for the two wing leading-edge sweep angles, the remainder of the discussion will be based on the configuration with the canard on.

A summary of the longitudinal aerodynamic characteristics of the configuration with and without the horizontal tail is shown in figure 19. These data for the configuration with the canard and horizontal-tail surfaces indicate that although the stability level for the 35° and 75° sweptback wings is essentially the same, the overall stability variation with wing sweep is 11.1 percent $\bar{c}$, with the maximum stability level occurring for the 60° sweptback wing. Also shown in this figure is the stability level occurring at a Mach number of 2.86 (taken from ref. 13). The change between the stability level of the 35° sweptback wing at a Mach number of 0.267 and that of the 75° sweptback wing at a Mach number of 2.86 is 7.9 percent $\bar{c}$. These data also show that removing the horizontal tail not only decreases the stability level of the configuration as expected, but also reverses the stability level at the wing sweep angles of 35° and 75°; that is, the 75° sweptback wing is now approximately 4 percent $\bar{c}$ less stable than the 35° sweptback wing. By taking into consideration changes in the area of the fore wing, the pivot location, and the relative motion between the fore wing and the main wing, improvements in the stability variation with wing leading-edge sweep angle and Mach number may be obtained.

Summary data comparing nacelles and engine pack arrangements are presented in figure 20. The configuration utilizing the four nacelles had the lower values of maximum untrimmed lift-drag ratio.

In order to determine the degree to which the double inboard pivot controls the stability variation with wing sweep, two fore wings of different areas were added ahead of the 35° sweptback wing as shown in figure 3. The effect of the addition of these fore wings on the longitudinal aerodynamic characteristics is shown in figure 21. The data indicate that small changes in the lift coefficient are obtained up to an angle of attack of about 8°; above this angle of attack, large increments in lift coefficient are obtained. This increase in lift coefficient at the higher angles of attack is due primarily to the nonlinear lift-curve slopes exhibited by these fore wings. The effect of these fore wings on the variation of the pitching-moment coefficient with angle of attack is shown in figure 22. These data, which have all been transferred to approximately the same stability level through zero lift coefficient, show that the larger the area of the the fore wing the more nonlinear is the variation of pitching-moment coefficient with angle of attack. Although large increases in the lift coefficient at the higher angles of attack can be obtained by the addition of these fore wings, figure 23 shows that there also will be an accompanying increase in the minimum drag, a decrease in the maximum untrimmed lift-drag ratio, and a forward movement of the aerodynamic center.

A portion of the data obtained in this fore-wing investigation was applied to the configuration (without the canard), shown in figure 2(a), and is presented in figure 24. This figure shows the variation of the static margin with wing sweep

for the configuration when the fore wing is retracted into the fuselage and for the configuration when the fore wing remains in the extended position as the main wing is swept forward. The fore-wing area is 27 percent of the reference area. These data indicate that a decrease of 6.5 percent $\bar{c}$ can be obtained in the static margin by retracting this fore wing into the fuselage as the main wing is swept forward from the 75° to the 35° sweptback position.

SUMMARY OF RESULTS

An investigation to determine the effect of a double-inboard-pivot variable-sweep wing on the low-speed longitudinal stability characteristics of a supersonic transport model configuration indicates the following results:

1. There is essentially no change in the stability level of the 35° and 75° sweptback wing positions. The change between the stability level of the 35° sweptback wing at a Mach number of 0.267 and that of the 75° sweptback wing at a Mach number of 2.86 is 7.9 percent of the mean aerodynamic chord.

2. The static margin is 6.5 percent of the mean aerodynamic chord less when the fore wing is retracted into the fuselage than when the fore wing remains in the extended position, as the main wing is swept forward from the 75° to the 35° sweptback positions.

3. The addition of the chord extension to the main-wing panel of the configuration with the wing in the 35° sweptback position leads to acceptable pitching-moment variations with angle of attack.

Langley Research Center,
National Aeronautics and Space Administration,
Langley Station, Hampton, Va., September 19, 1962.

REFERENCES

1. Staff of Langley Research Center: The Supersonic Transport - A Technical Summary. NASA TN D-423, 1960.

2. Carraway, Ausley B., Gregory, Donald T., and Carmel, Melvin M.: An Exploratory Investigation of a Transport Configuration Designed for Supersonic Cruise Flight Near a Mach Number of 3. NASA TM X-216, 1960.

3. Vogler, Raymond D., and Turner, Thomas R.: Exploratory Low-Speed Wind-Tunnel Stability Investigation of a Supersonic Transport Configuration With Variable-Sweep Wings. NASA TM X-597, 1961.

4. Morris, Owen G., Carmel, Melvin M., and Carraway, Ausley B.: An Investigation at Mach Numbers From 0.20 to 4.63 of the Aerodynamic Performance, Static Stability, and Trimming Characteristics of a Canard Configuration Designed for Efficient Supersonic Cruise Flight. NASA TM X-617, 1961.

5. Sleeman, William C., Jr., and Robins, A. Warner: Low-Speed Investigation of the Aerodynamic Characteristics of a Variable-Sweep Supersonic Transport Configuration Having a Blended Wing and Body. NASA TM X-619, 1961.

6. Carraway, Ausley B., Morris, Owen G., and Carmel, Melvin M.: Aerodynamic Characteristics at Mach Numbers From 0.20 to 4.63 of a Canard-Type Supersonic Commerical Air Transport Configuration. NASA TM X-628, 1962.

7. Kelly, Thomas C., Carmel, Melvin M., and Gregory, Donald T.: An Exploratory Investigation at Mach Numbers of 2.50 and 2.87 of a Canard Bomber-Type Configuration Designed for Supersonic Cruise Flight. NACA RM L58B28, 1958.

8. Baals, Donald T., Toll, Thomas A., and Morris, Owen G.: Airplane Configurations for Cruise at a Mach Number of 3. NACA RM L58E14a, 1958.

9. Gregory, Donald T., and Carraway, Ausley B.: Investigation of the Effects of Engine Arrangement on Stability and Performance Characteristics of a Canard-Type Aircraft Configuration Near a Mach Number of 3 Including Effects of Canard Plan Form. NASA TM X-217, 1960.

10. Alford, William J., Jr., and Henderson, William P.: An Exploratory Investigation of the Low-Speed Aerodynamic Characteristics of Variable-Wing-Sweep Airplane Configurations. NASA TM X-142, 1959.

11. Polhamus, Edward C., and Hammond, Alexander D.: Aerodynamic Research Relative to Variable-Sweep Multimission Aircraft. Ch. II of Compilation of Papers Summarizing Some Recent NASA Research on Manned Military Aircraft. NASA TM X-420, 1960, pp. 13-38.

12. Polhamus, Edward C., Alford, William J., Jr., and Foster, Gerald V.: Subsonic and Supersonic Aerodynamic Characteristics of an Airplane Configuration Utilizing Double-Pivot Variable-Sweep Wings. NASA TM X-743, 1963.

13. Shaw, David S., and Henderson, William P.: Wind-Tunnel Investigation at Mach Numbers From 1.60 to 2.86 of the Static Aerodynamic Characteristics of a Supersonic Transport Configuration With Variable-Sweep Wings Employing a Double Inboard Pivot. NASA TM X-745, 1962.

TABLE I.- DIMENSIONS OF BASIC CONFIGURATION COMPONENTS

Fuselage:	
Length, in.	41.64
Maximum width, in.	2.65
Maximum height, in.	2.30
Fineness ratio	16.52
Canard:	
Leading-edge sweep angle, deg	60.00
Trailing-edge sweep angle, deg	0
Tip chord, in.	0.400
Root chord, in.	5.600
Root chord (exposed), in.	3.890
Area (total), sq ft	0.125
Area (exposed), sq ft	0.0596
Aspect ratio (total)	2.00
Horizontal tail:	
Leading-edge sweep angle, deg	60.00
Trailing-edge sweep angle, deg	37.50
Tip chord, in.	2.208
Root chord, in.	6.308
Root chord (exposed), in.	5.300
Area (total), sq ft	0.252
Area (exposed), sq ft	0.1642
Span, in.	8.516
Aspect ratio	2.00
Vertical tail:	
Leading-edge sweep angle, deg	60.00
Trailing-edge sweep angle, deg	37.50
Tip chord, in.	2.208
Root chord (exposed), in.	6.308
Span, in.	4.258

Wing:	$\Lambda = 75^\circ$	$\Lambda = 60^\circ$	$\Lambda = 45^\circ$	$\Lambda = 35^\circ$
Fore-wing sweep angle, deg	79.75	84.00	No fore wing	No fore wing
Main-wing trailing-edge sweep angle, deg	65.35	50.35	35.35	25.35
Area (includes fore wing where applicable), sq ft	1.285	1.151	0.892	0.885
Span, in.	16.528	23.780	29.740	32.70
Mean aerodynamic chord, in.	13.789	9.281	4.725	4.201
Aspect ratio (includes fore wing)	1.476	3.413	6.884	8.394

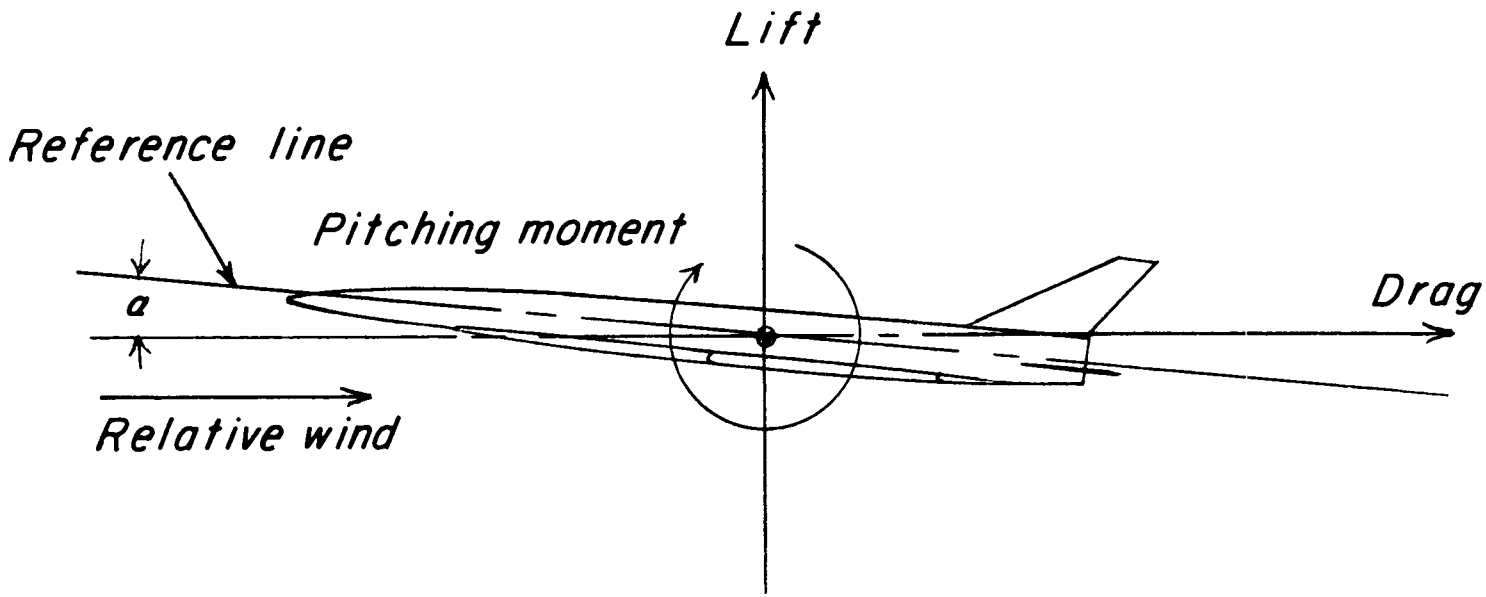

Figure 1.- System of axes used in presentation of data. Arrows indicate positive direction of forces and pitching moment.

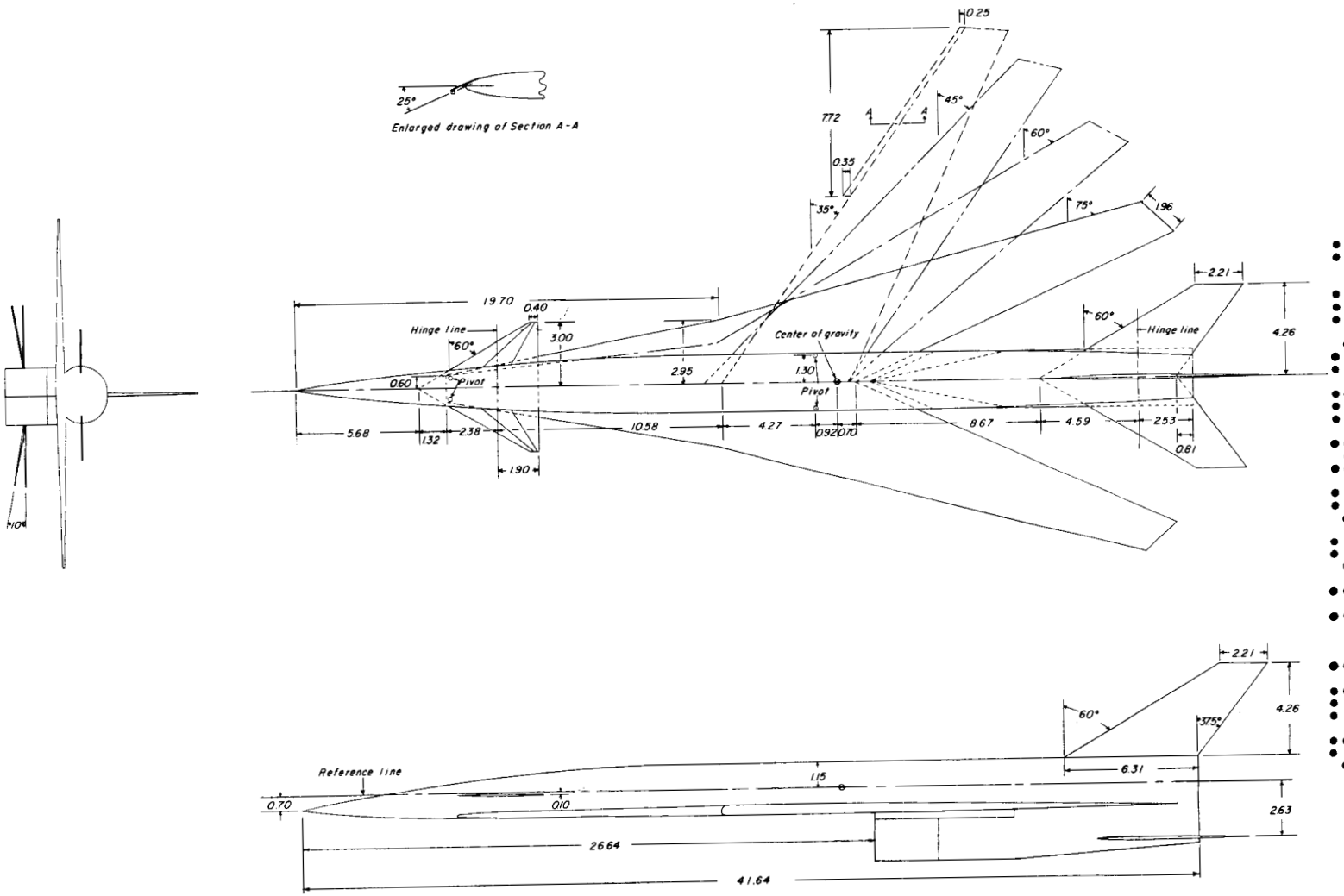

(a) Model with engine pack.

Figure 2.- Drawings and dimensions of model. All dimensions are in inches.

[redacted]

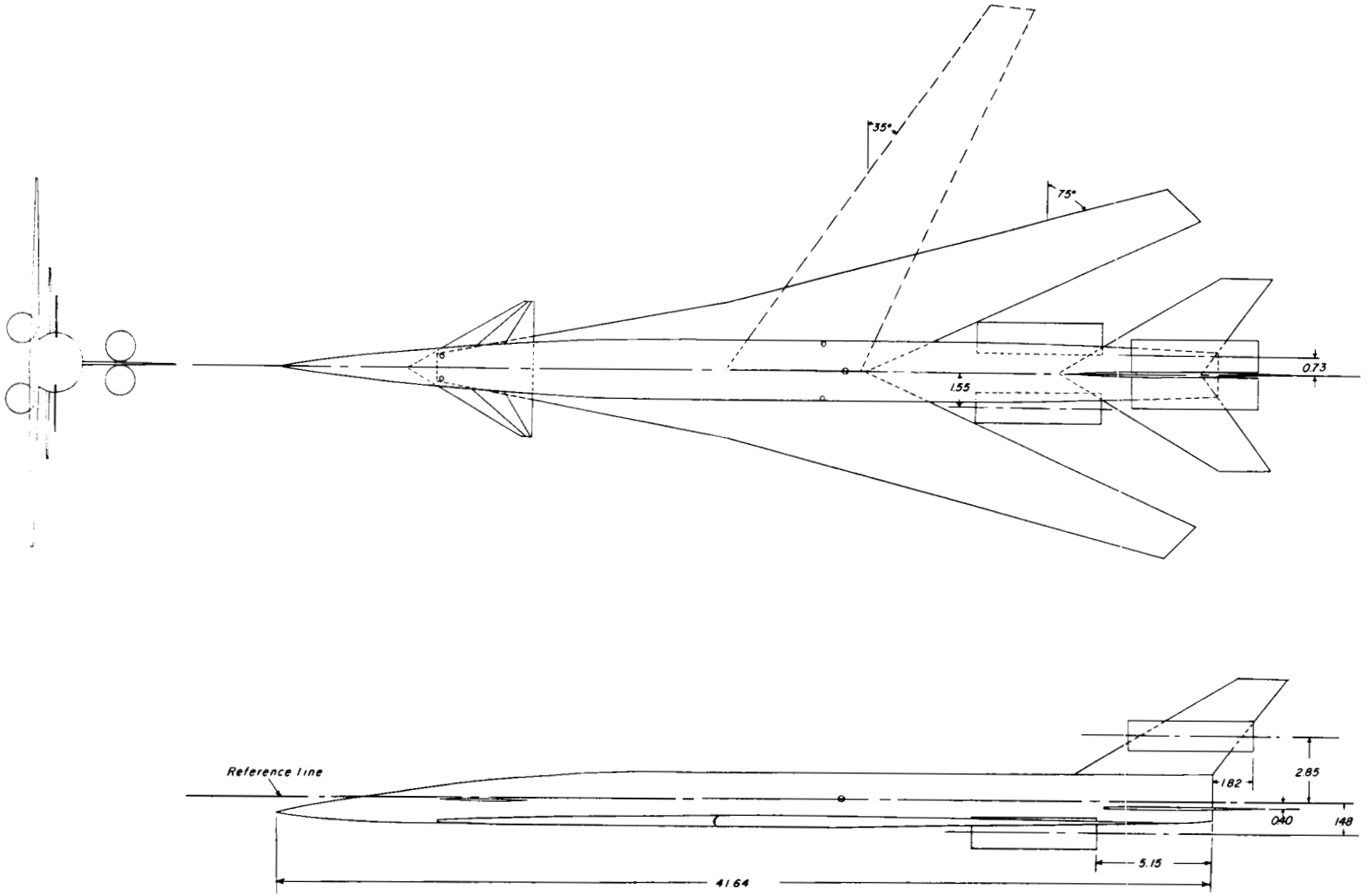

(b) Model with four nacelles.

Figure 2.- Continued.

[redacted]

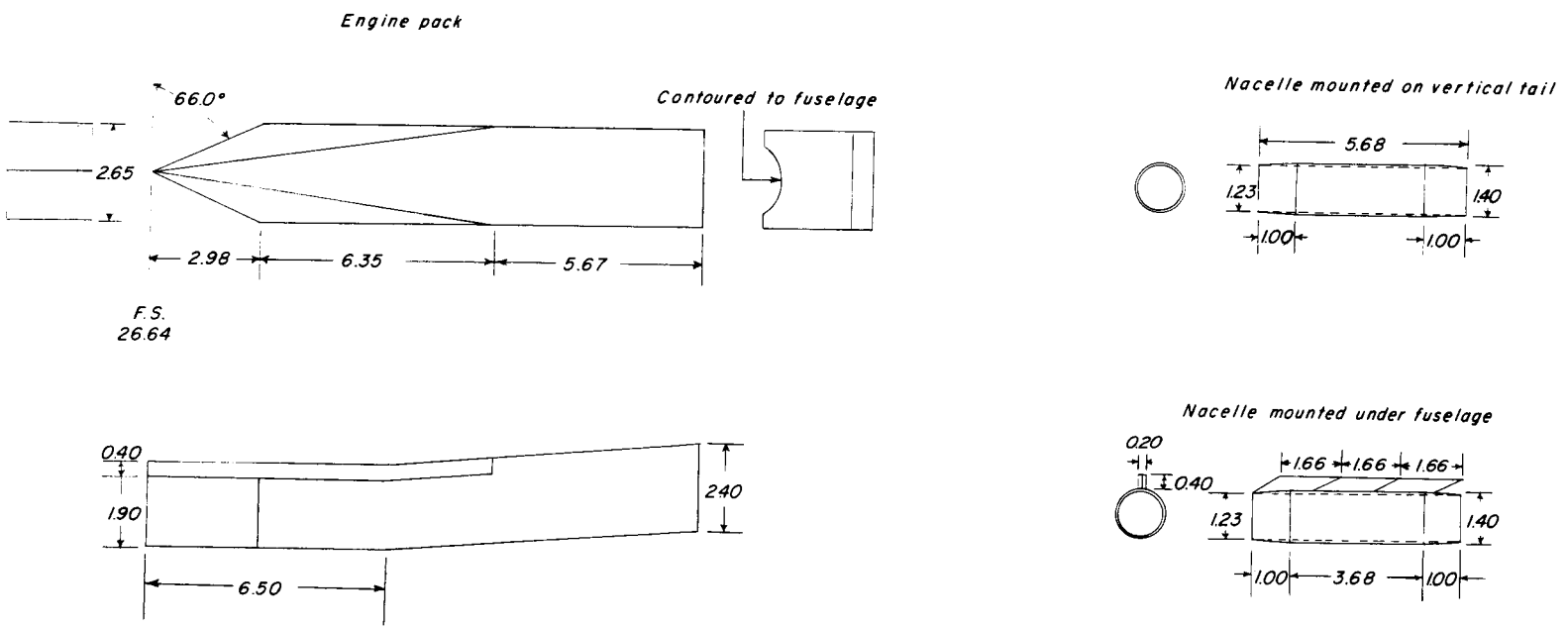

(c) Details of engine pack and nacelles.

Figure 2.- Concluded.

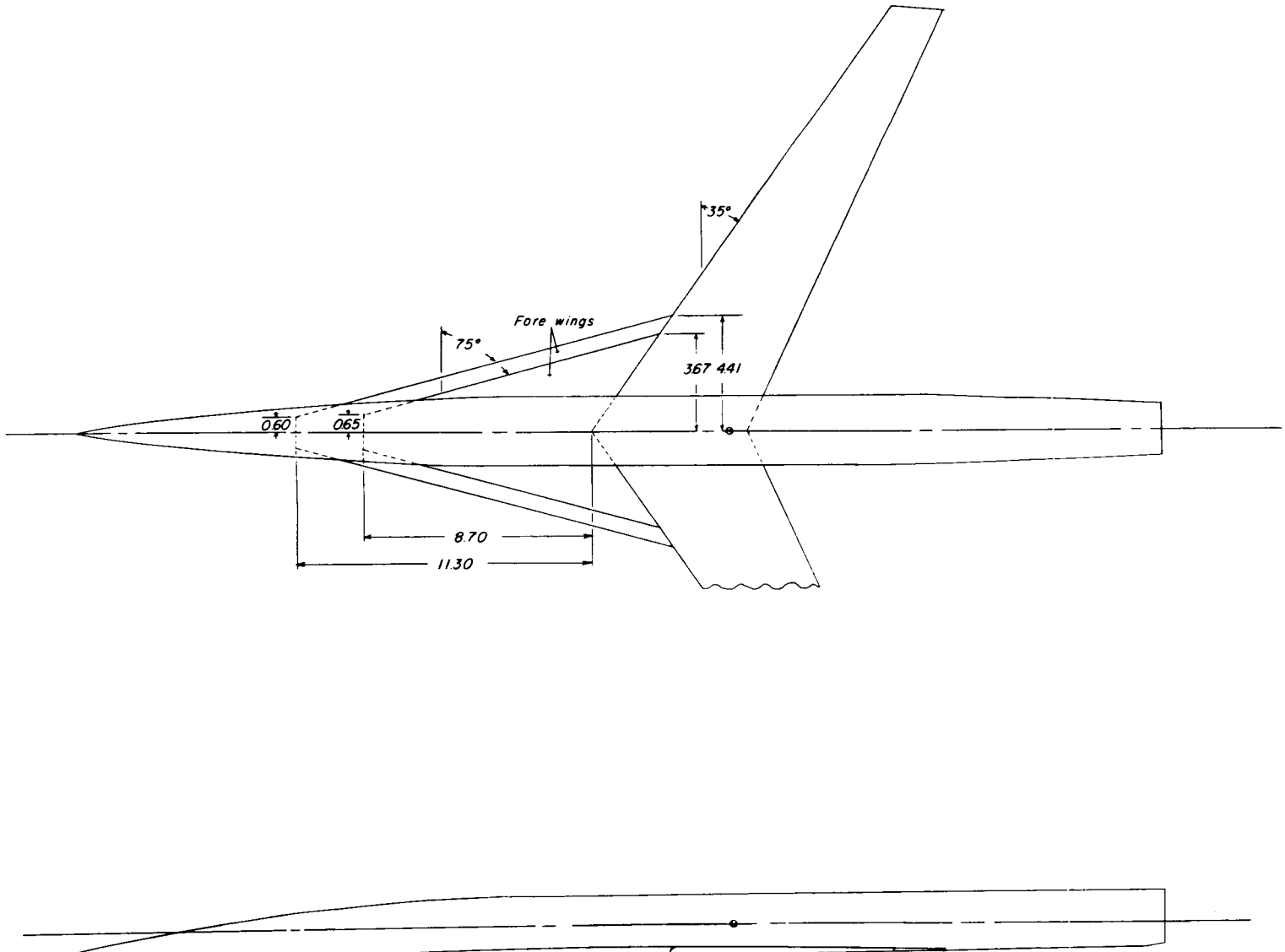

Figure 3.- Details of fore wings.

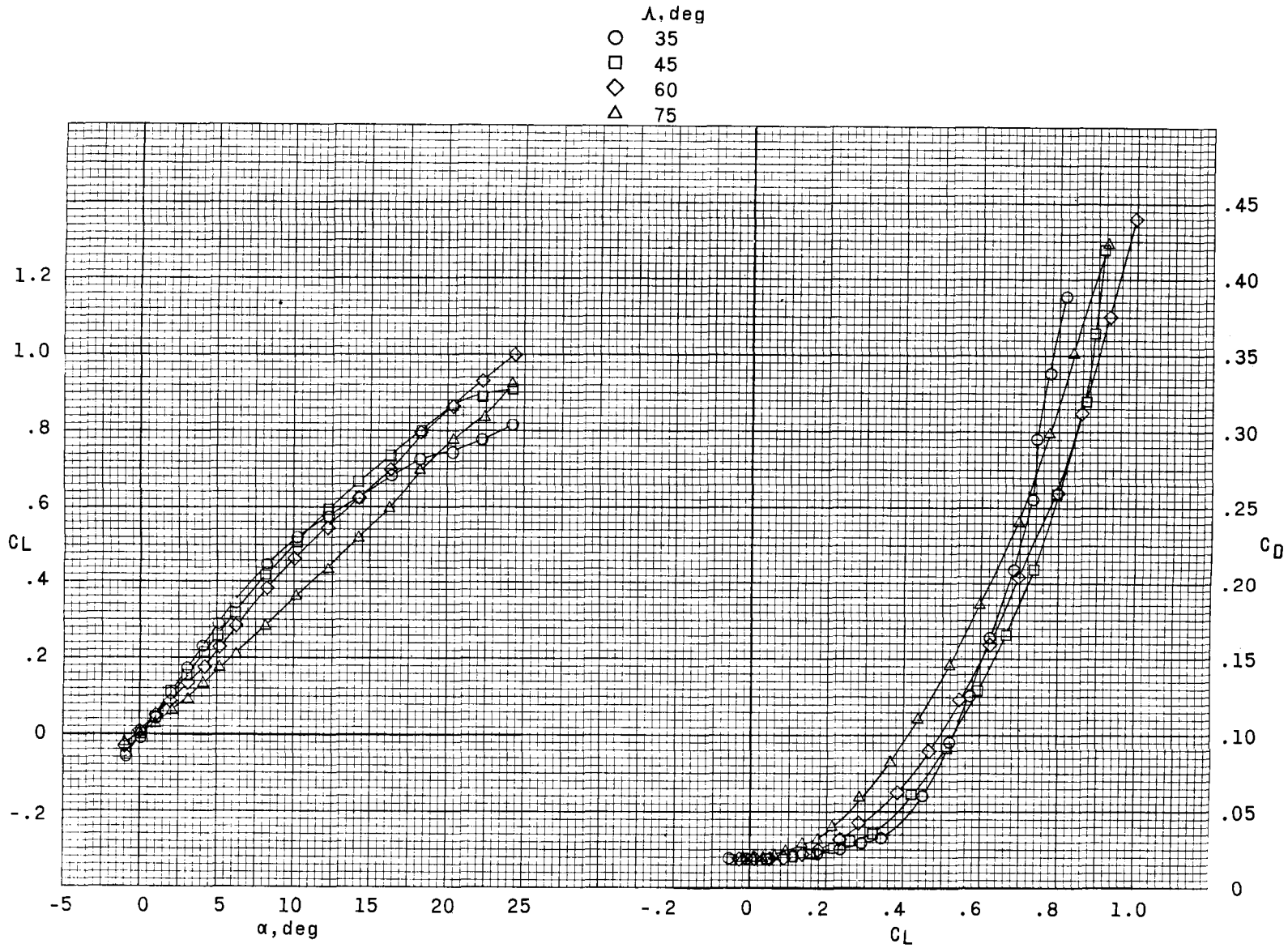

Figure 4.- Effect of wing leading-edge sweep angle on longitudinal aerodynamic characteristics of WFVHCE configuration. $\delta_c = 0^o$; $i_t = 0^o$; $\Gamma_t = 0^o$.

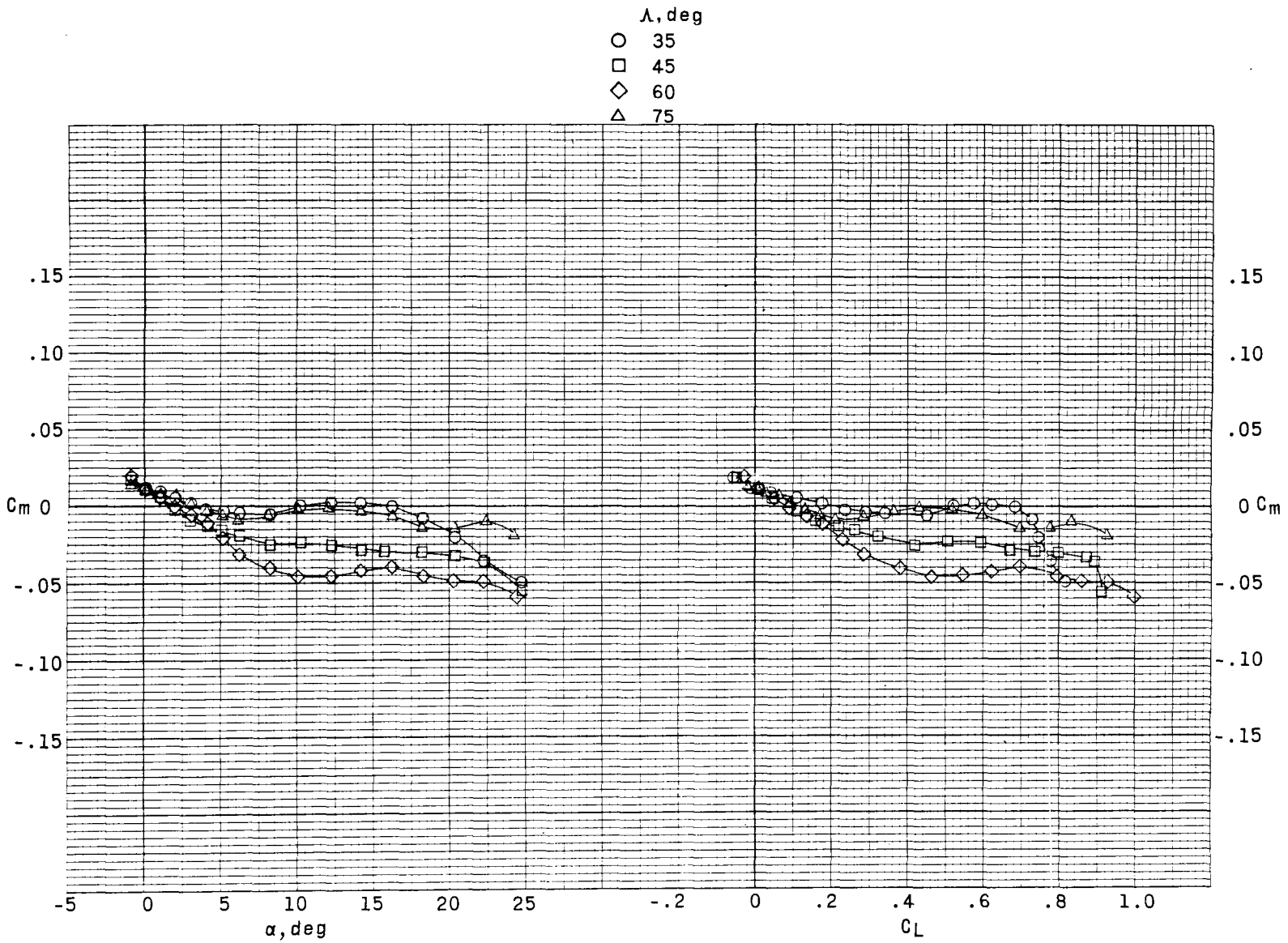

Figure 4.- Concluded.

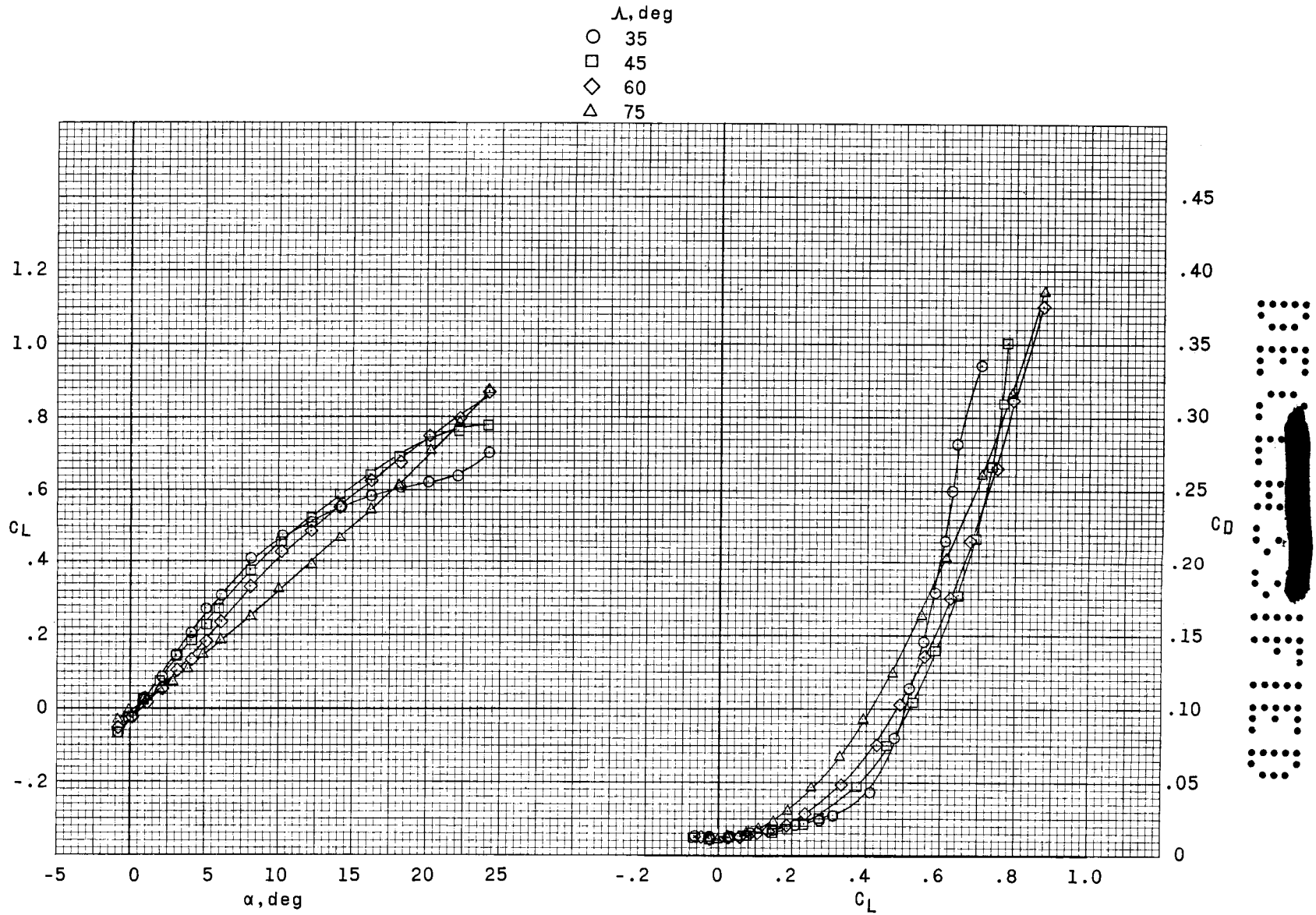

Figure 5.- Effect of wing leading-edge sweep angle on longitudinal aerodynamic characteristics of WFVH configuration. $i_t = 0^\circ$; $\Gamma_t = 0^\circ$.

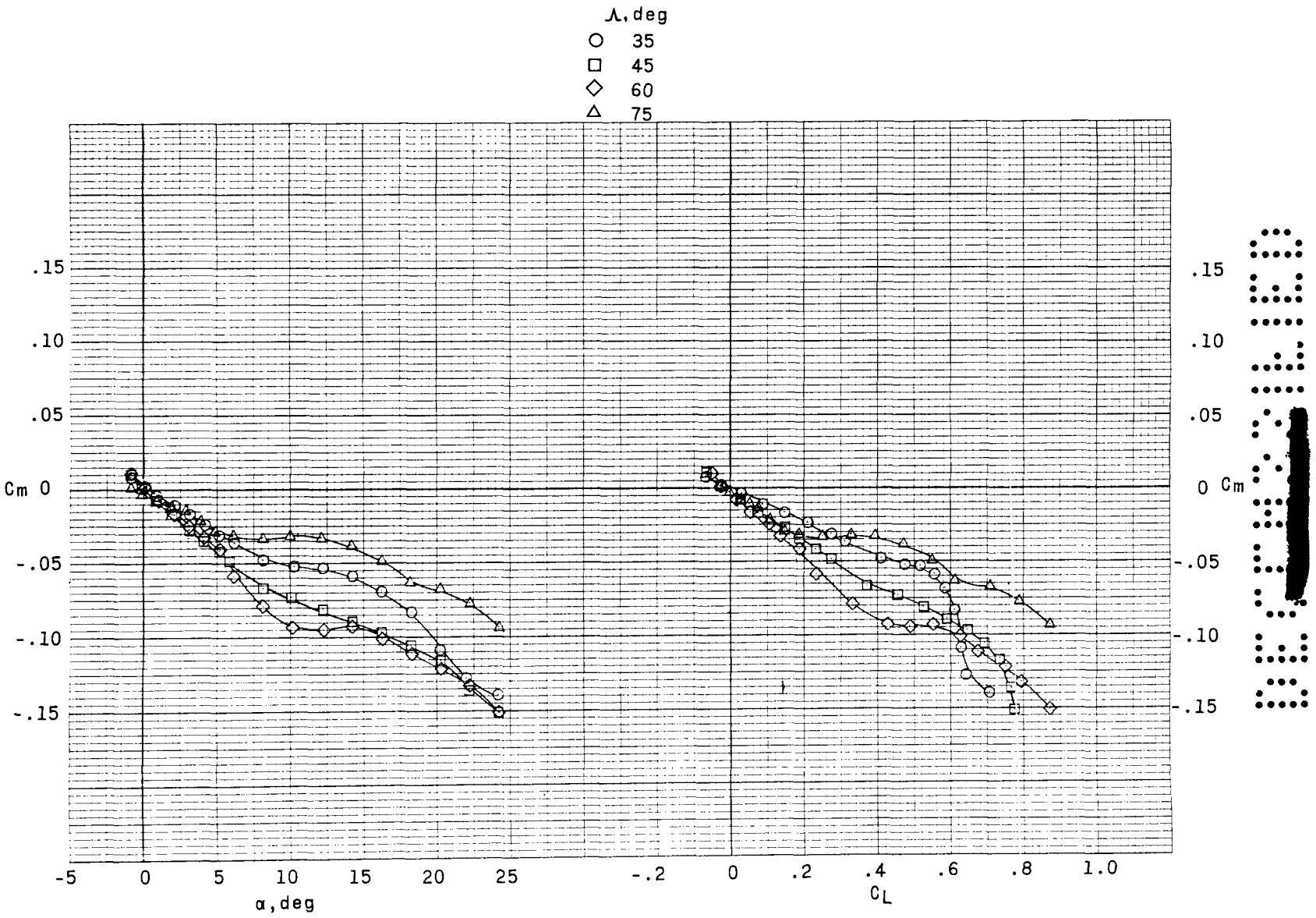

Figure 5.- Concluded.

[redacted]

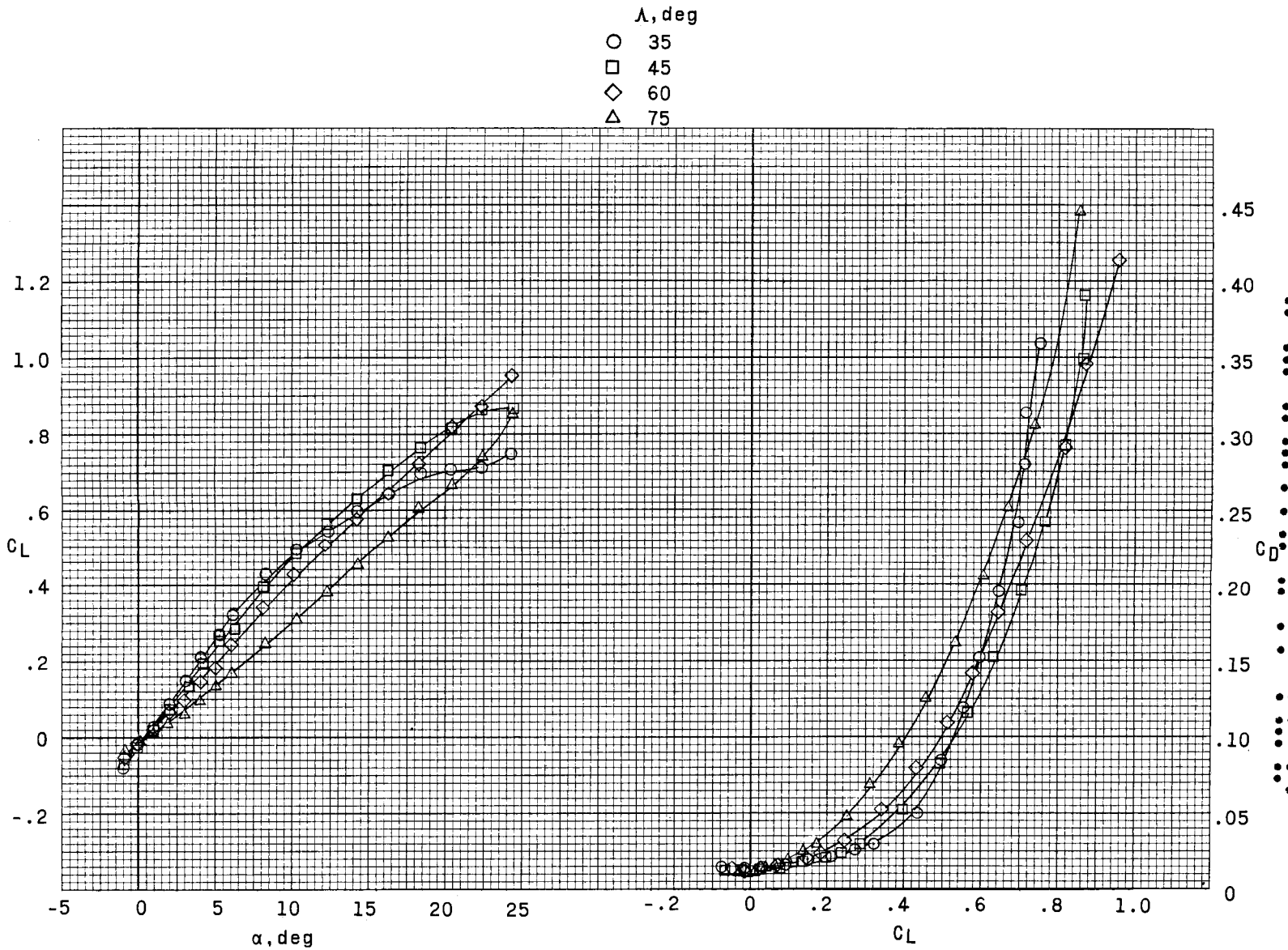

Figure 6.- Effect of wing leading-edge sweep angle on longitudinal aerodynamic characteristics of WFVHC configuration. $\delta_c = 0^o$; $i_t = 0^o$; $\Gamma_t = 0^o$.

[redacted]

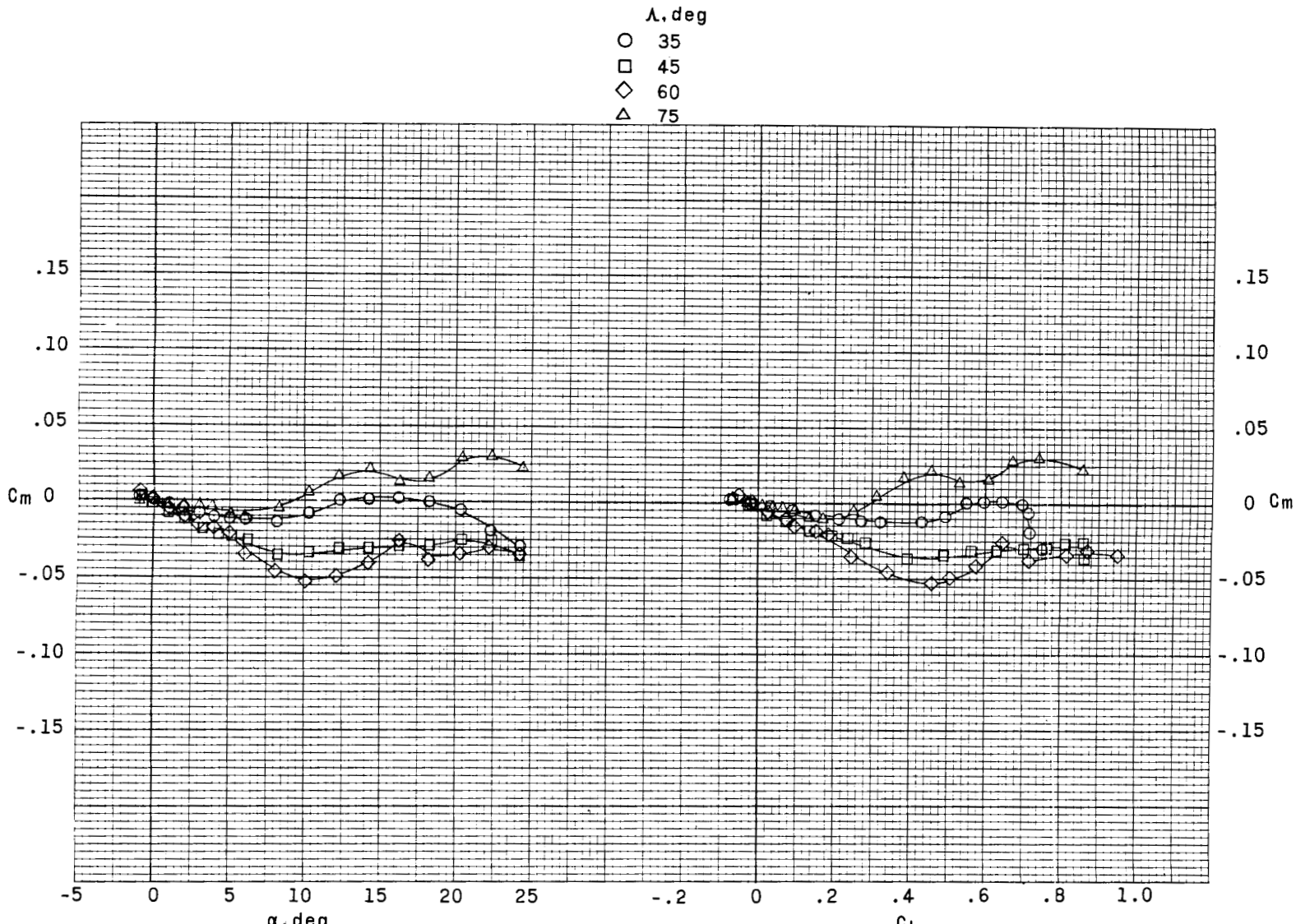

Figure 6.- Concluded.

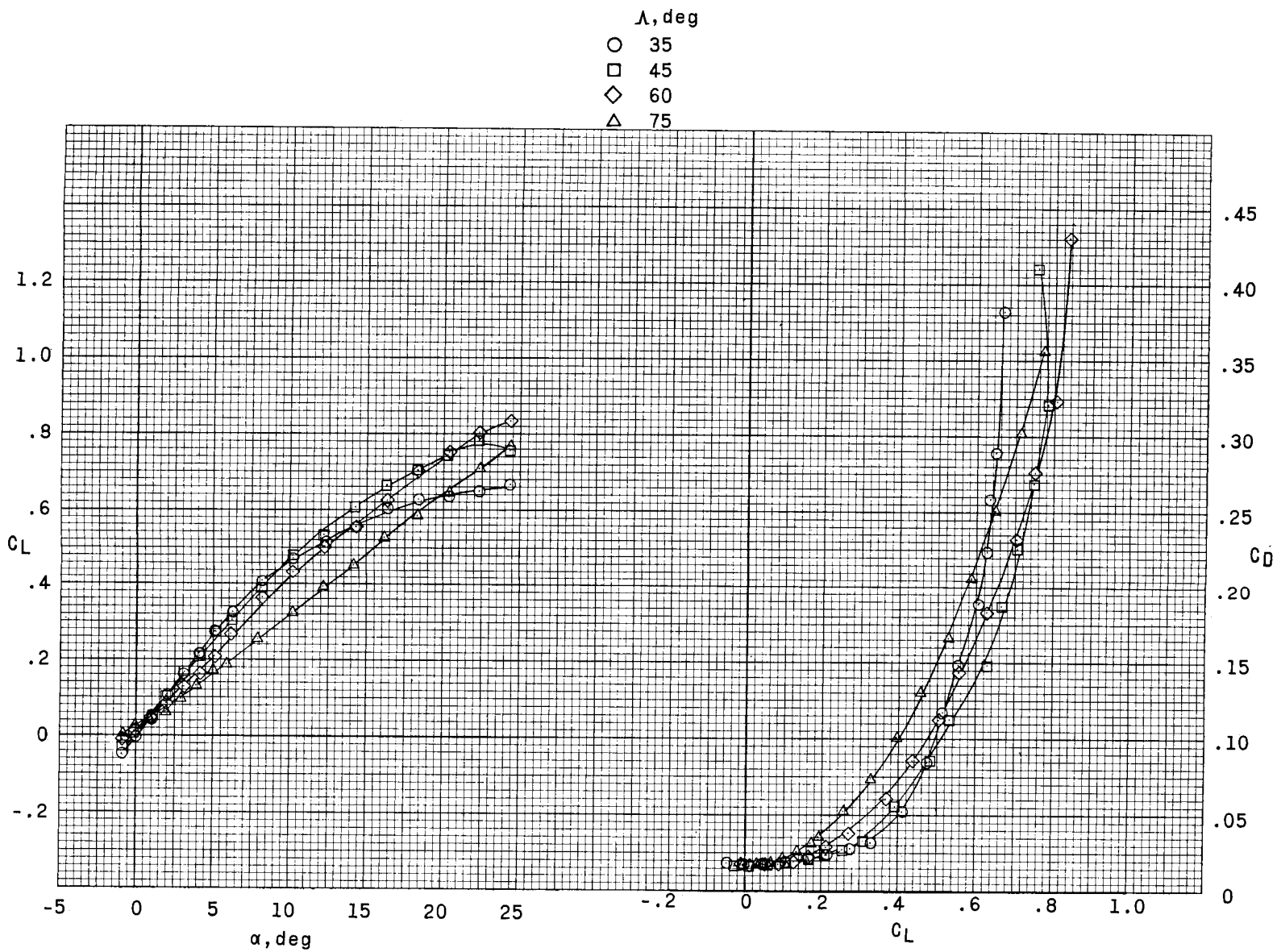

Figure 7.- Effect of wing leading-edge sweep angle on longitudinal aerodynamic characteristics of WFVCE configuration. $\delta_c = 0^{\circ}$.

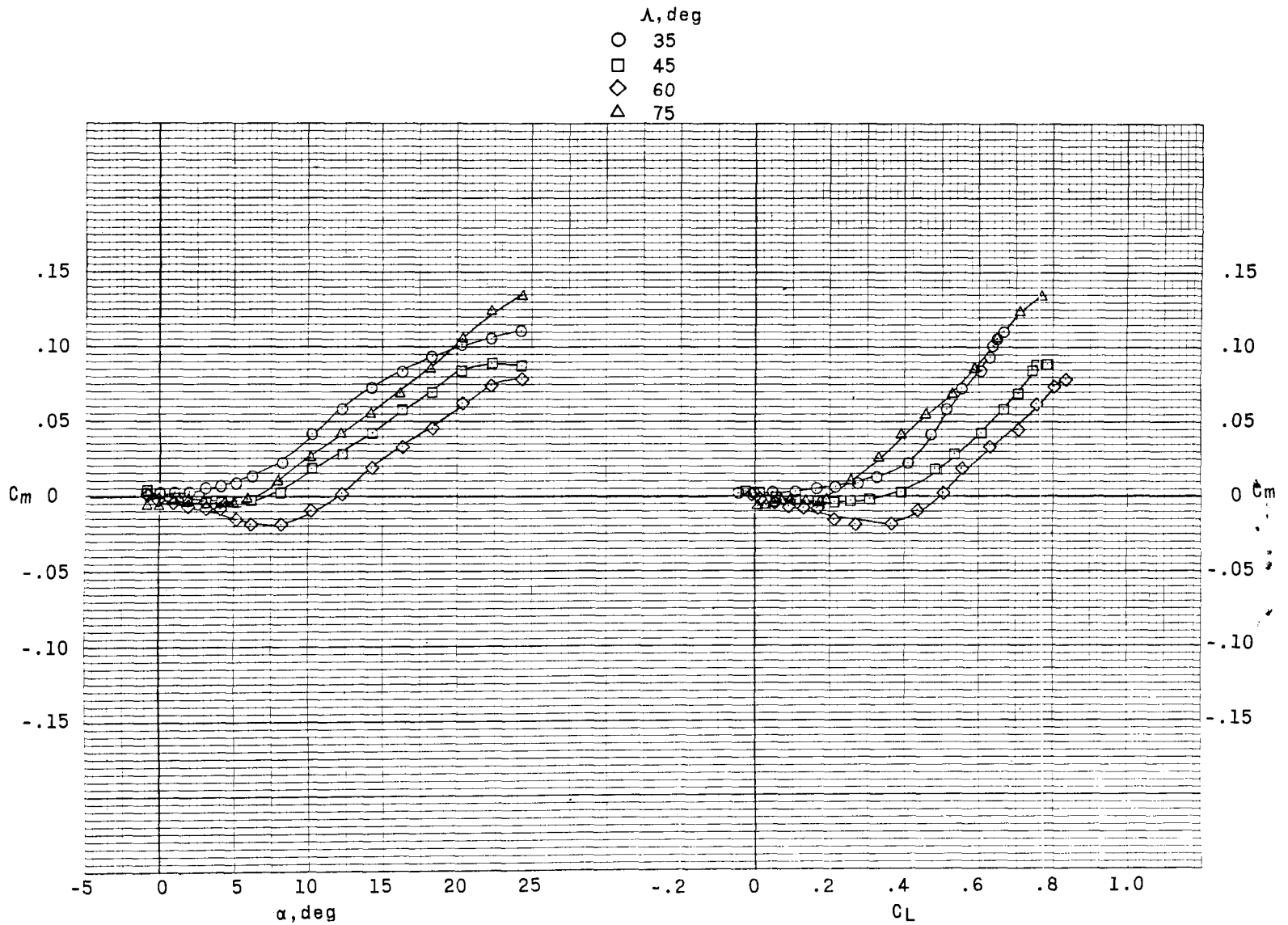

Figure 7.- Concluded.

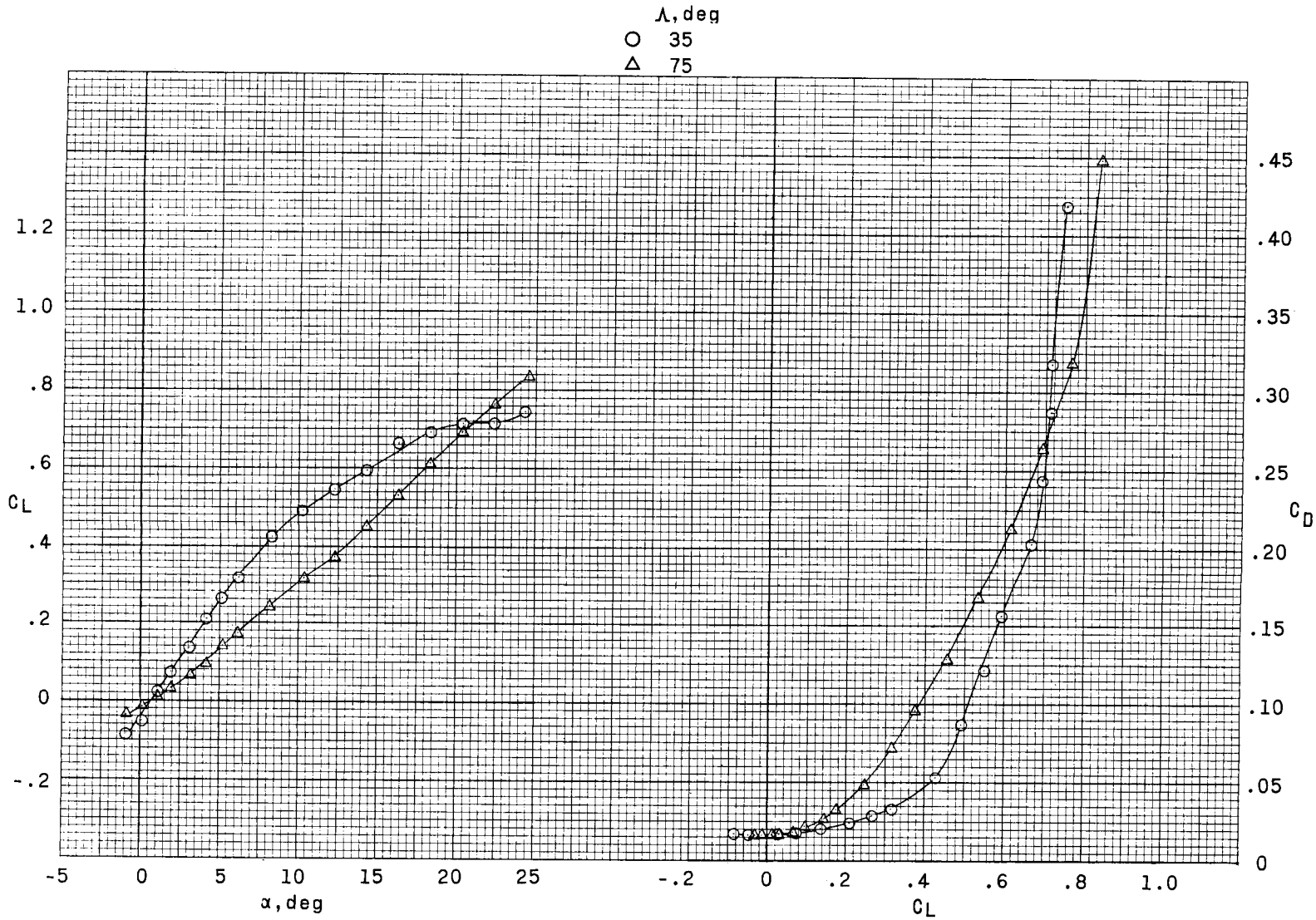

Figure 8.- Effect of wing leading-edge sweep angle on longitudinal aerodynamic characteristics of WFVHCN configuration. $\delta_c = 0^o$; $i_t = 0^o$; $\Gamma_t = 0^o$.

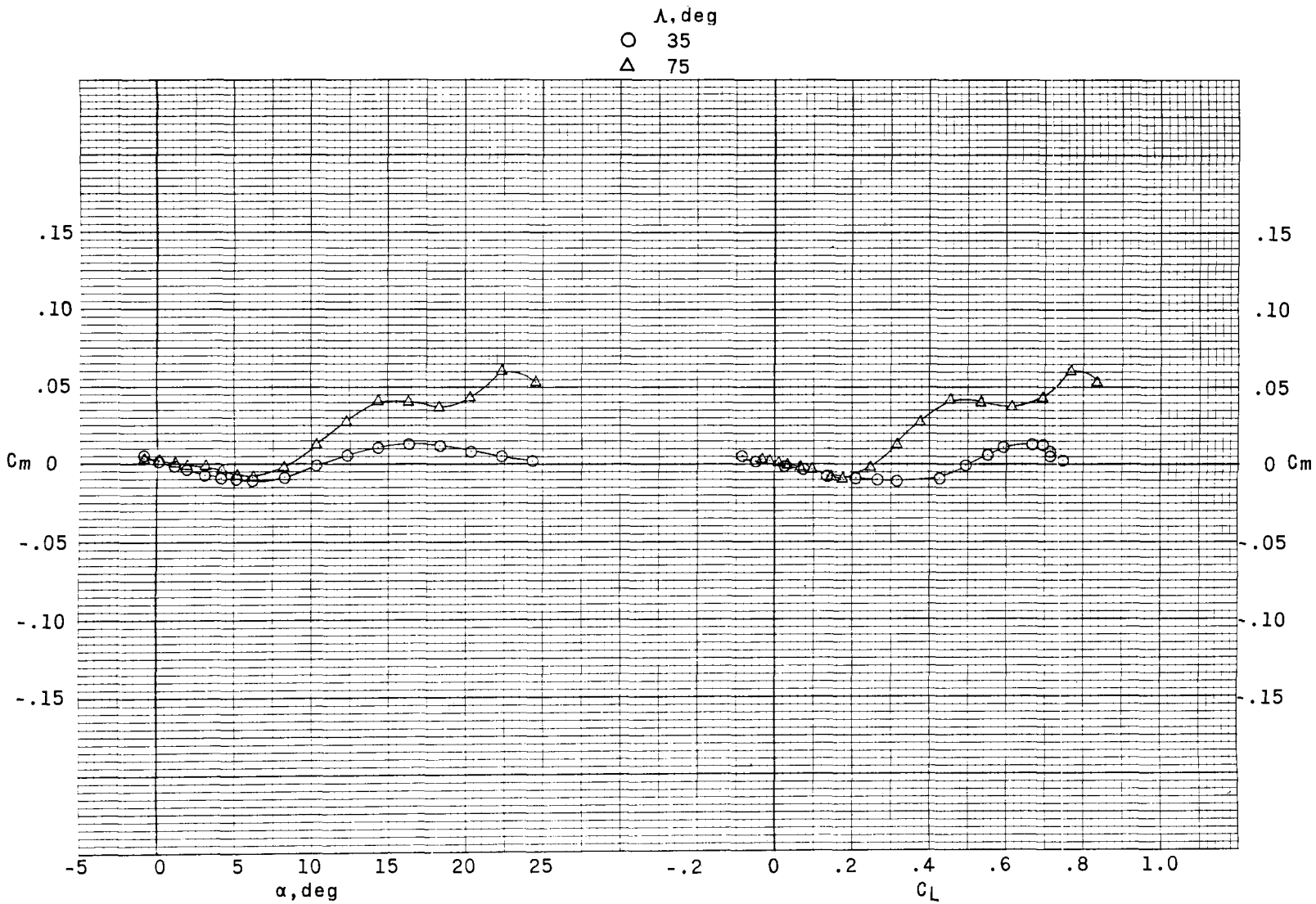

Figure 8.- Concluded.

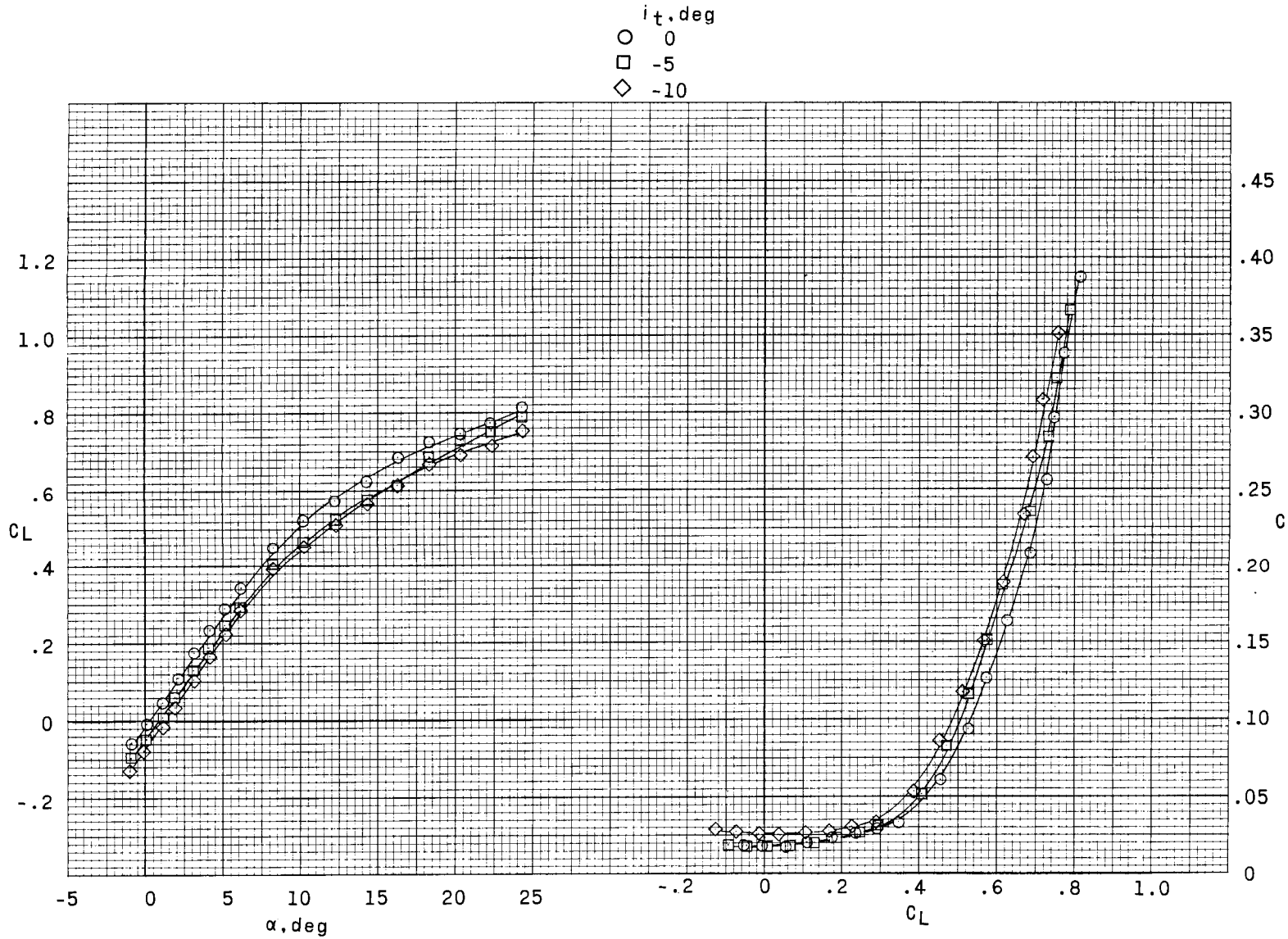

Figure 9.- Effect of horizontal-tail incidence on longitudinal aerodynamic characteristics of WFVHCE configuration. $\Lambda = 35^{\circ}$.

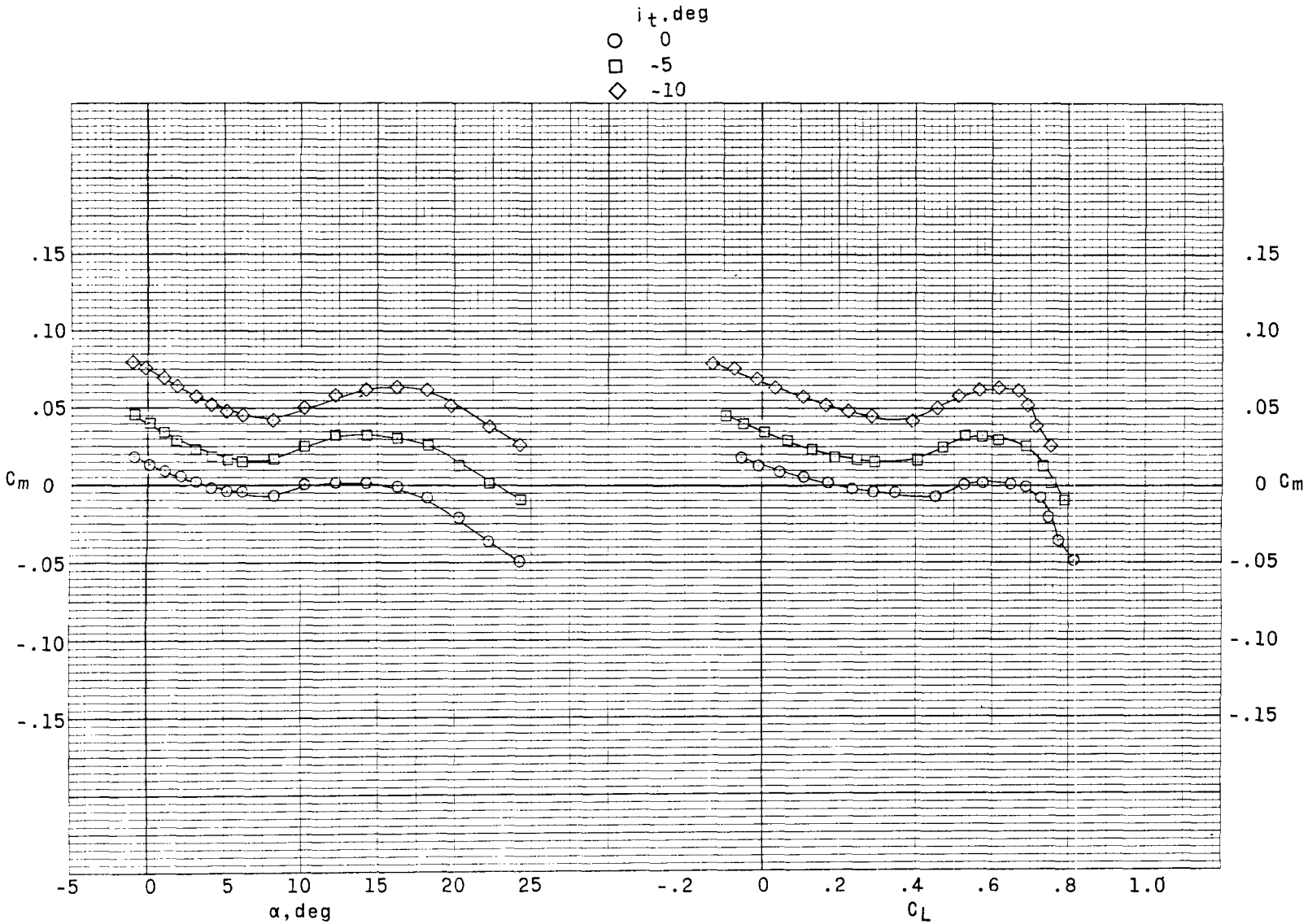

Figure 9.- Concluded.

L-3053

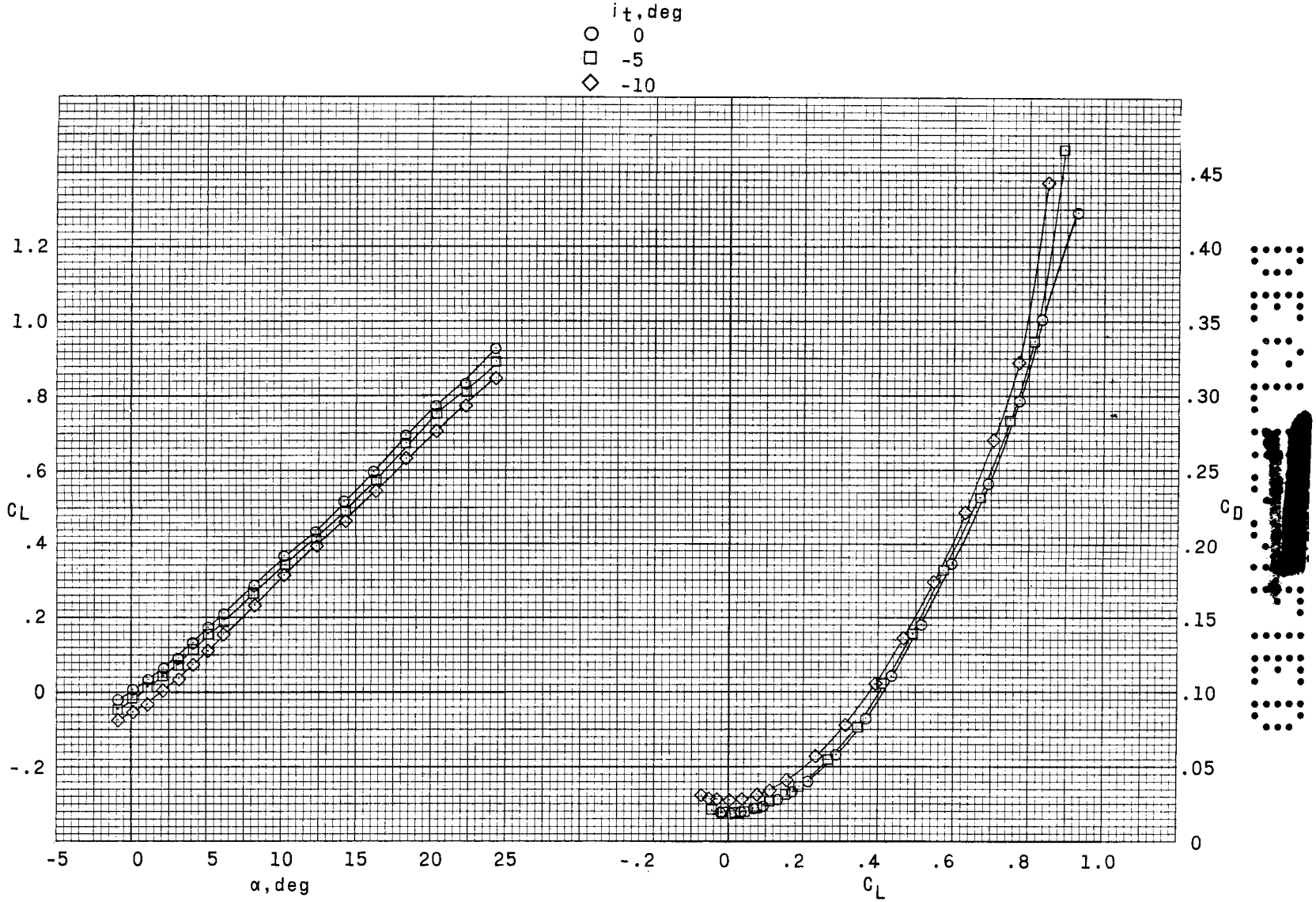

Figure 10.- Effect of horizontal-tail incidence on longitudinal aerodynamic characteristics of WFVHCE configuration. $\Lambda = 75^{\circ}$.

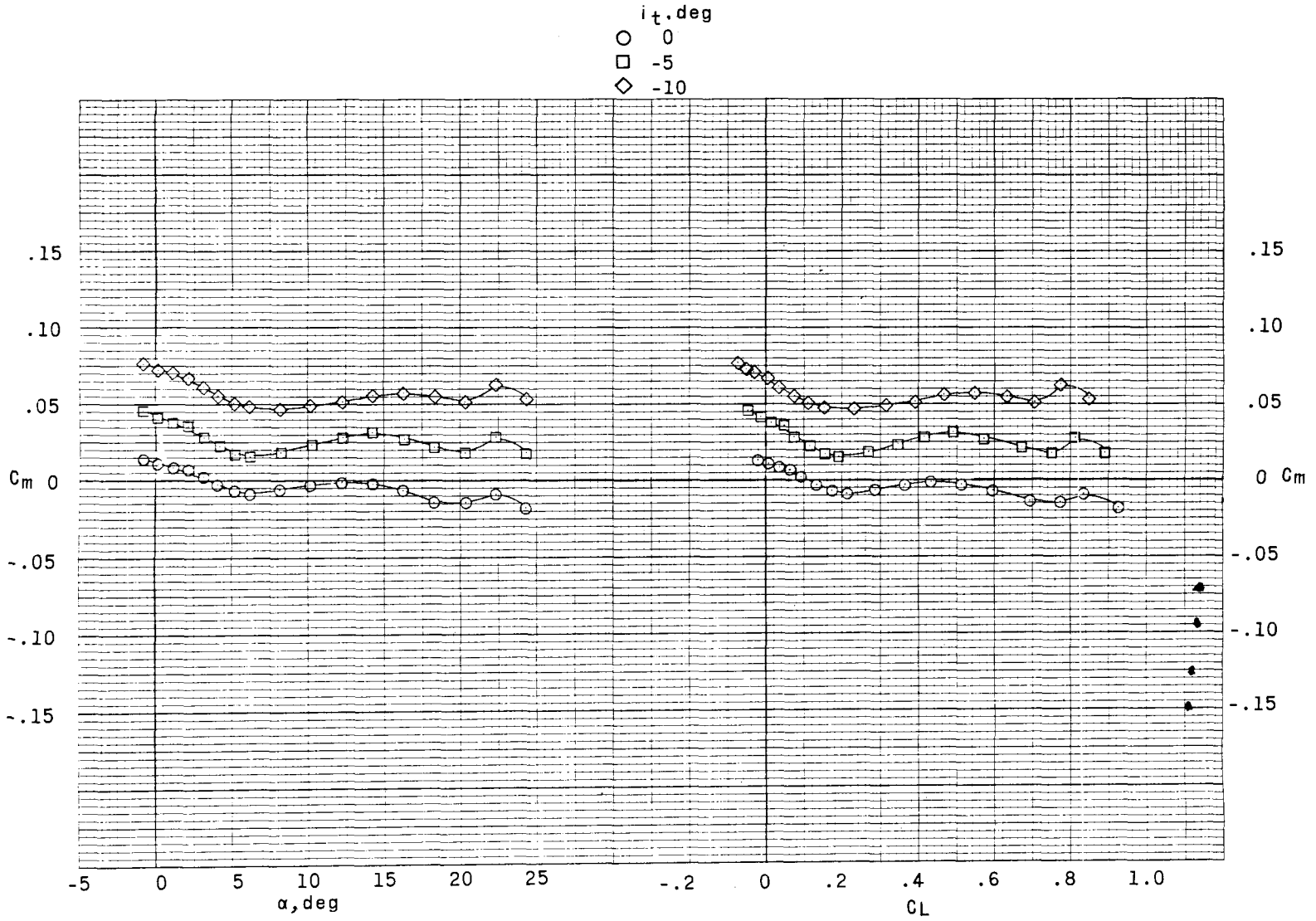

Figure 10.- Concluded.

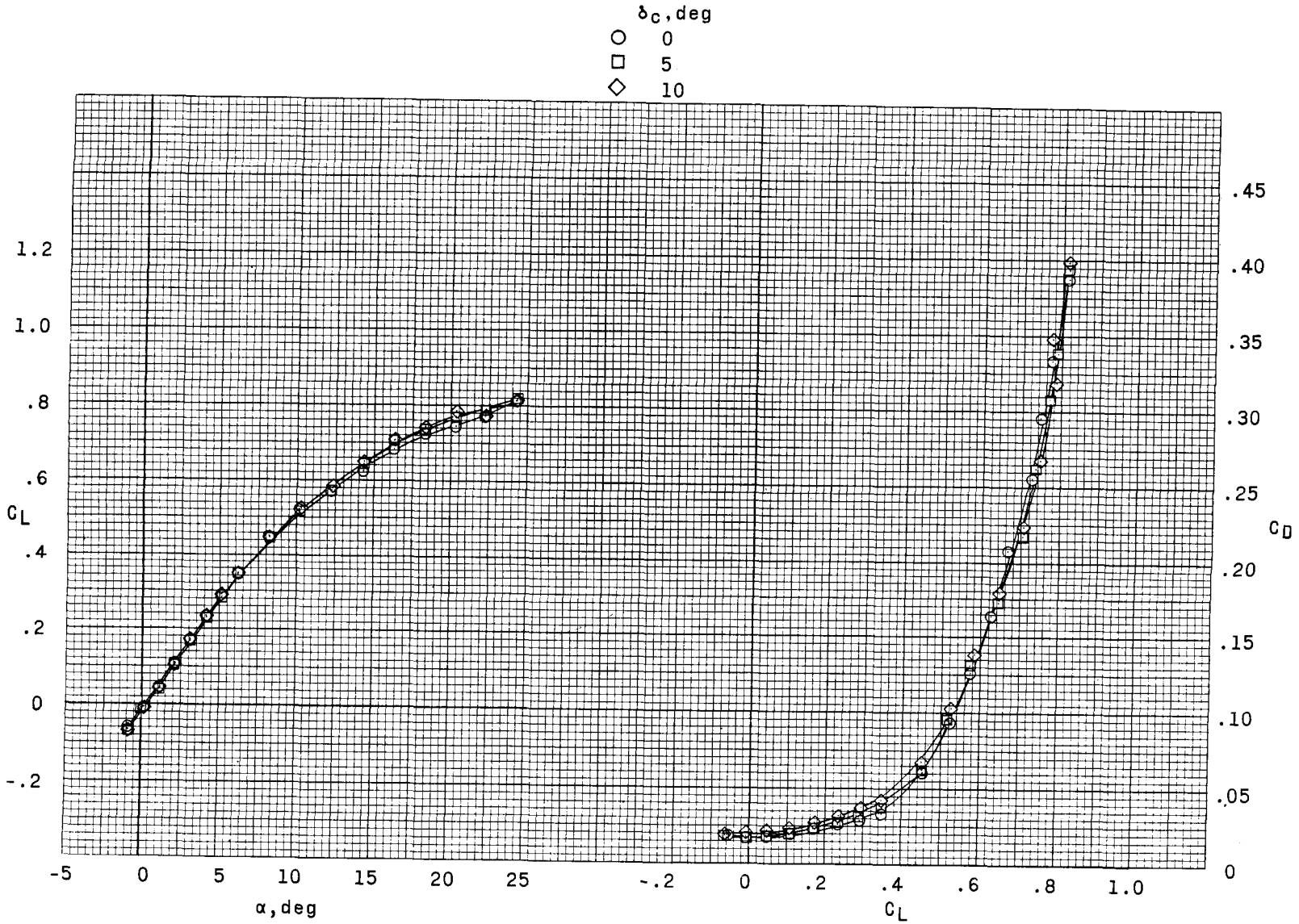

Figure 11.- Effect of canard deflection on longitudinal aerodynamic characteristics of WFVHCE configuration. $\Lambda = 35^{\circ}$; $i_t = 0^{\circ}$; $\Gamma_t = 0^{\circ}$.

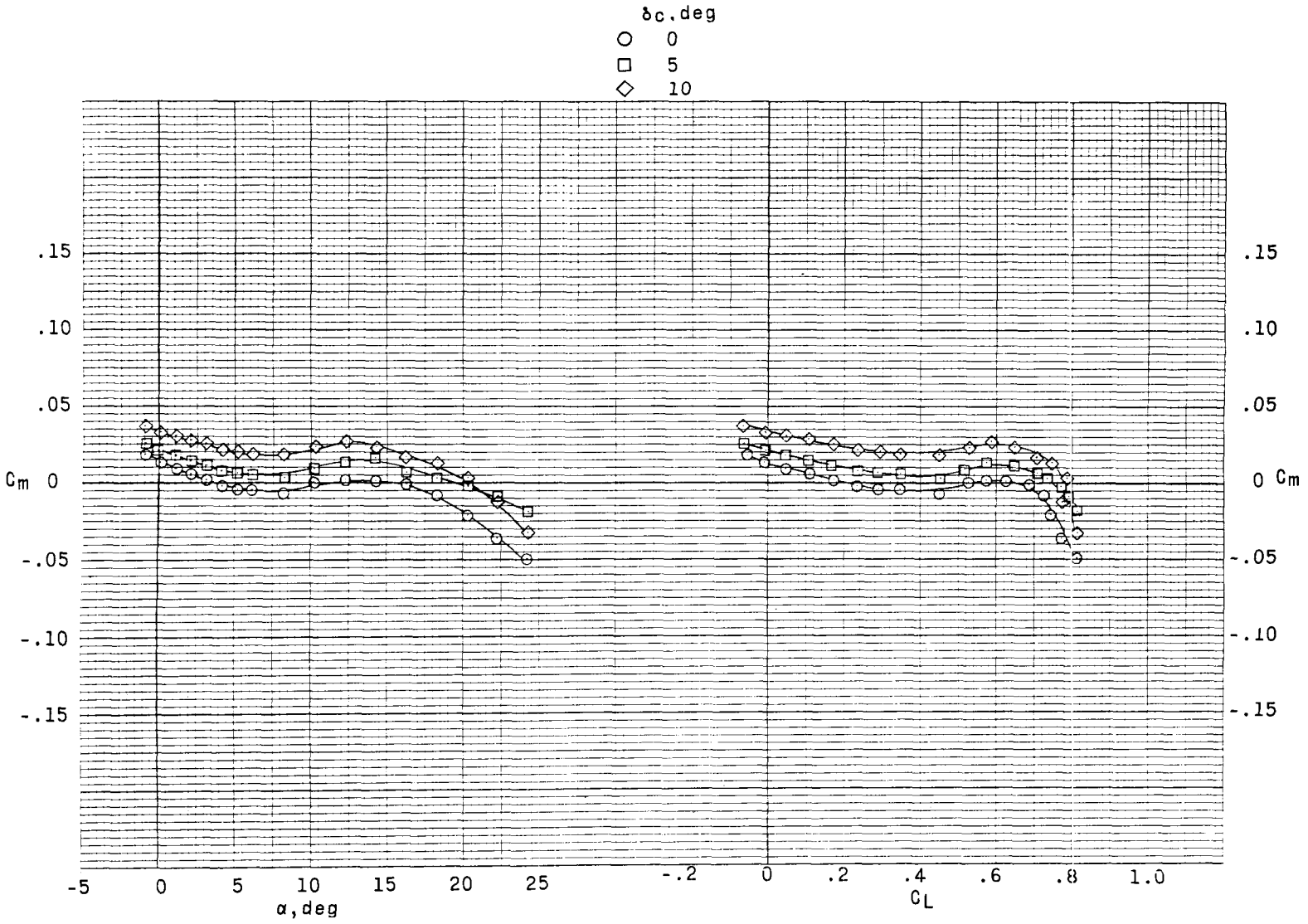

Figure 11.- Concluded.

[redacted]

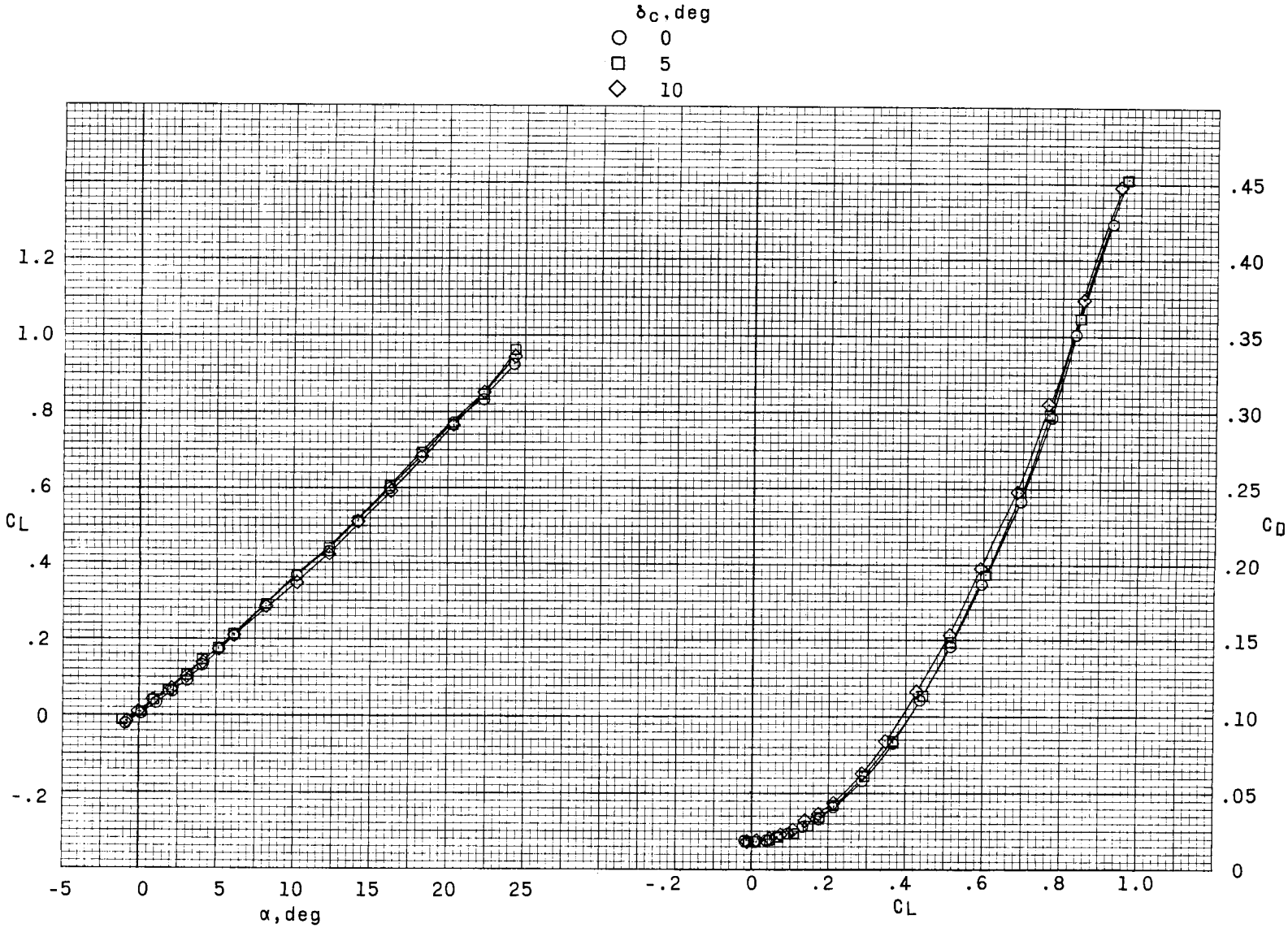

[redacted]

Figure 12.- Effect of canard deflection on longitudinal aerodynamic characteristics of WFVHCE configuration. $\Lambda = 75^{\circ}$; $i_t = 0^{\circ}$; $\Gamma_t = 0^{\circ}$.

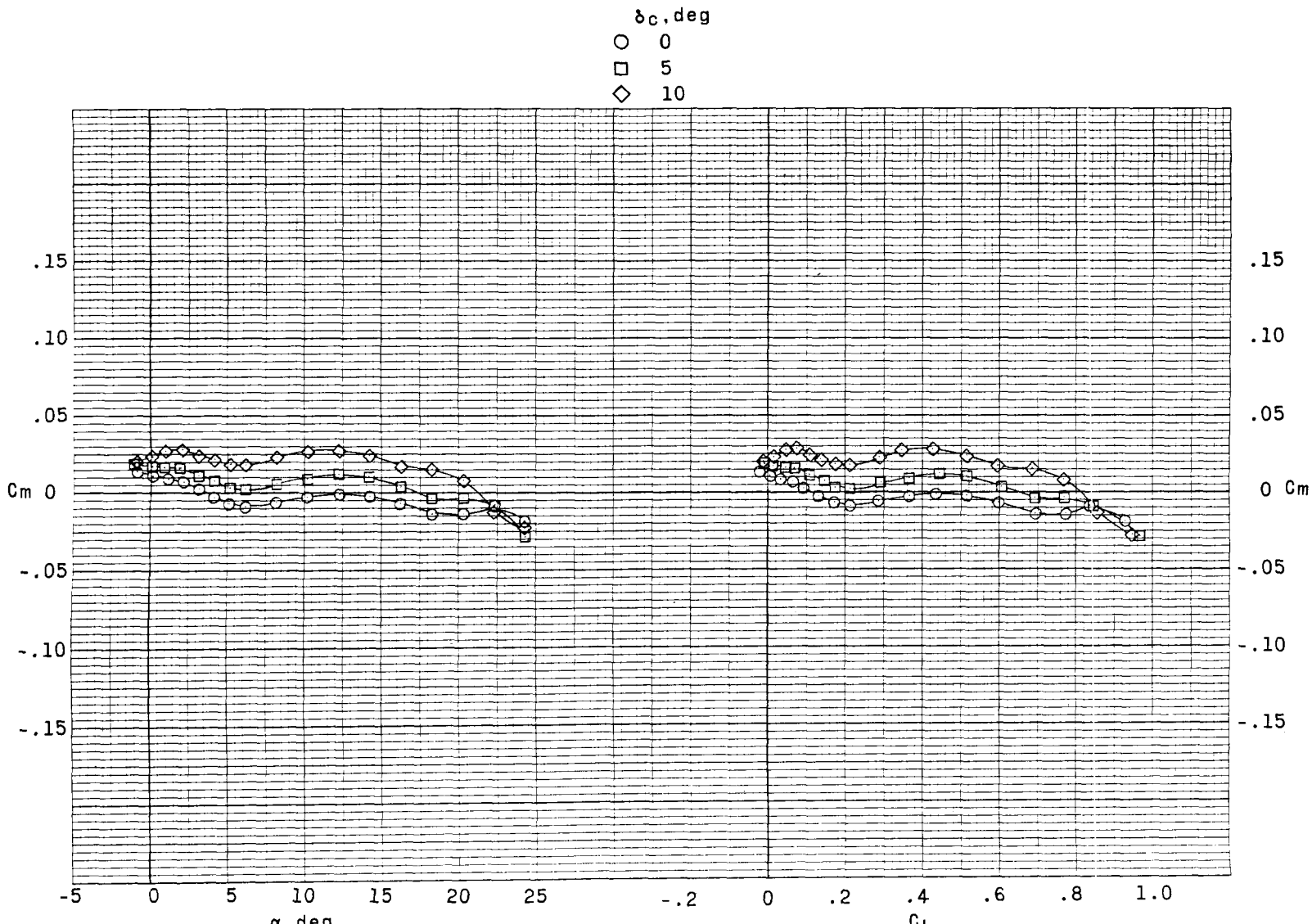

Figure 12.- Concluded.

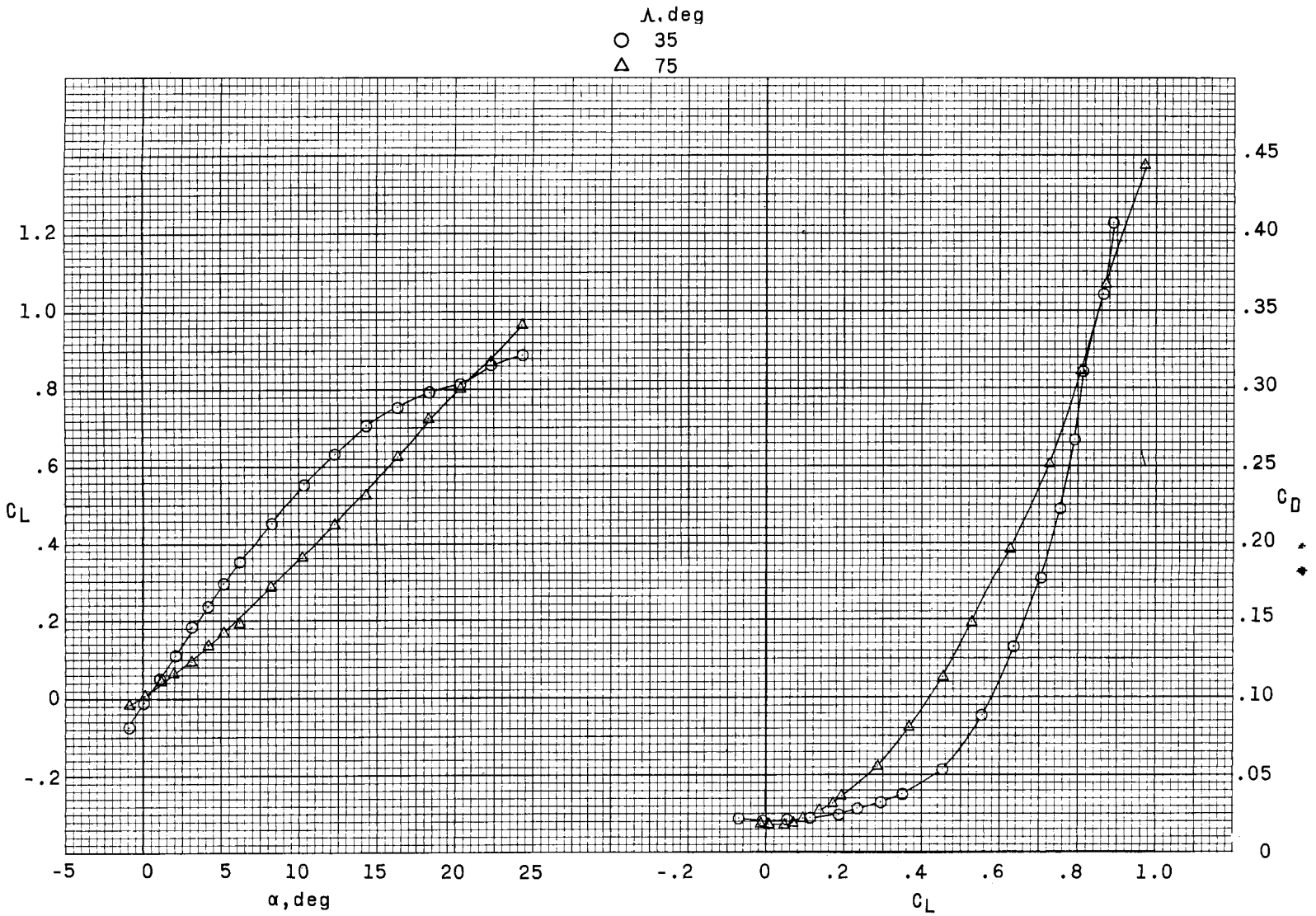

Figure 13.- Effect of wing leading-edge sweep angle on longitudinal aerodynamic characteristics of WFVHCE configuration with chord extension on main wing. $\delta_c = 0^\circ$; $i_t = 0^\circ$; $\Gamma_t = 0^\circ$.

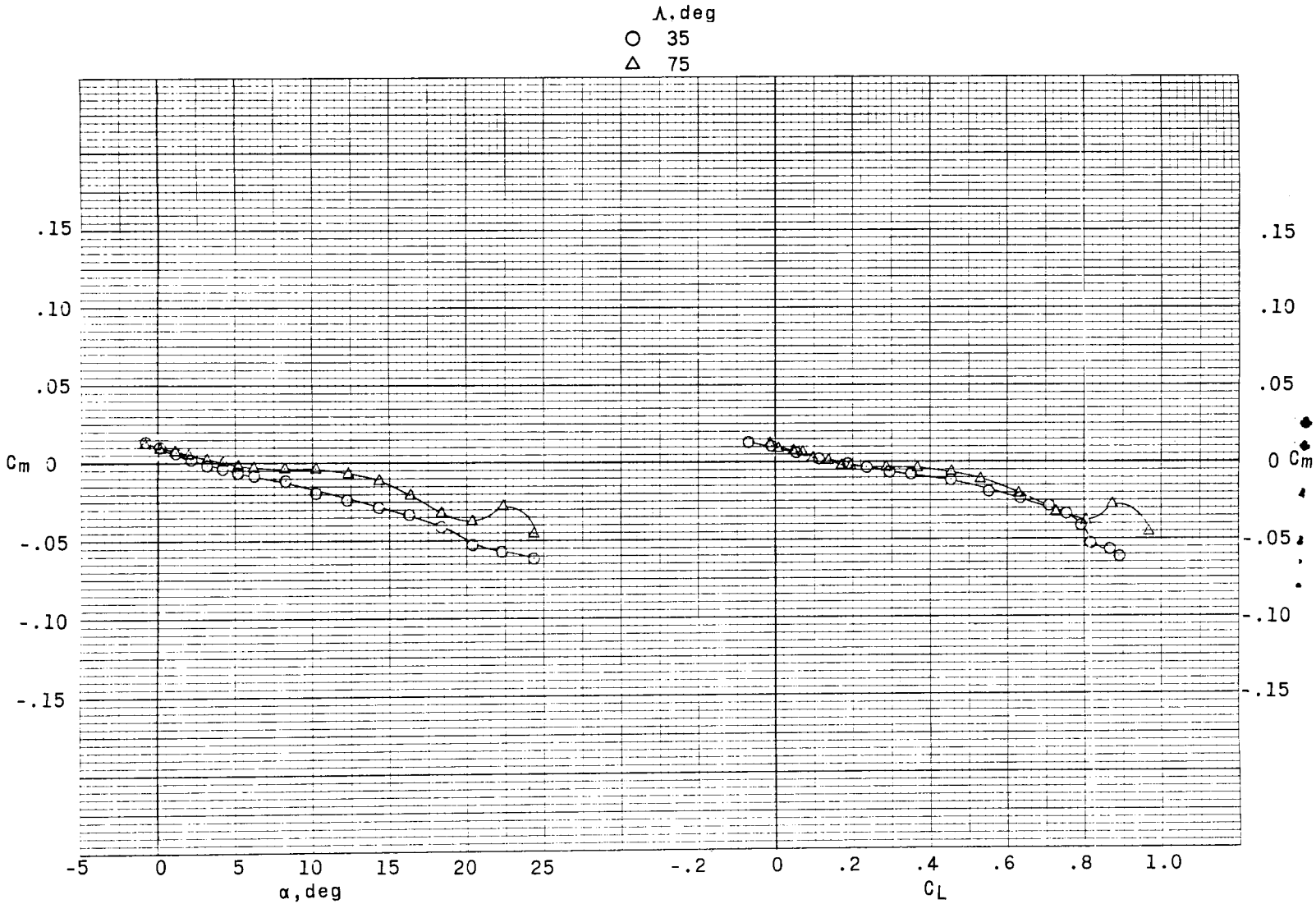

Figure 13.- Concluded.

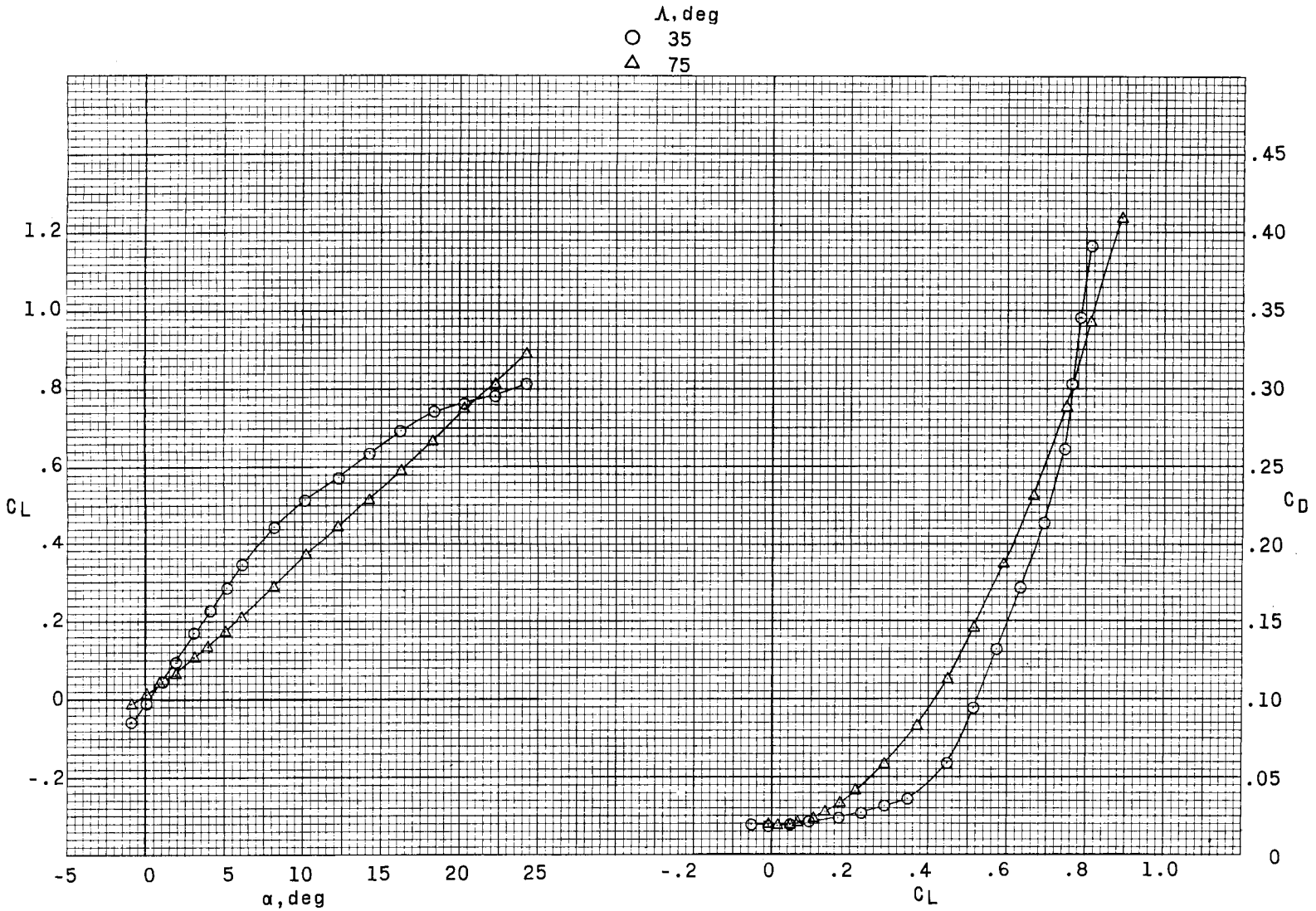

Figure 14.- Effect of wing leading-edge sweep angle on longitudinal aerodynamic characteristics of WFVHCE configuration with horizontal tail set at $\Gamma_t = 10^{\circ}$. $\delta_c = 0^{\circ}$; $i_t = 0^{\circ}$.

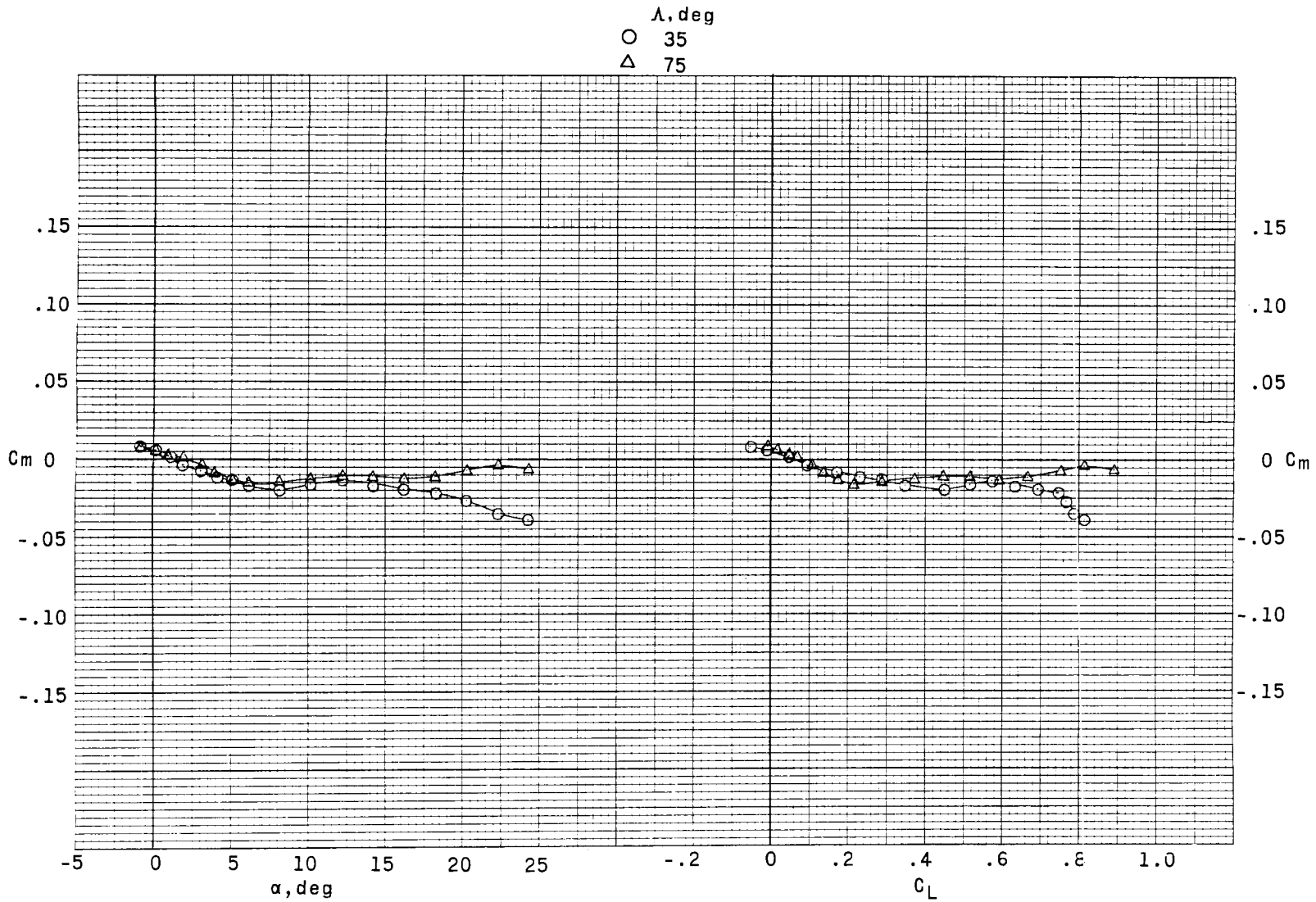

Figure 14.- Concluded.

[redacted]

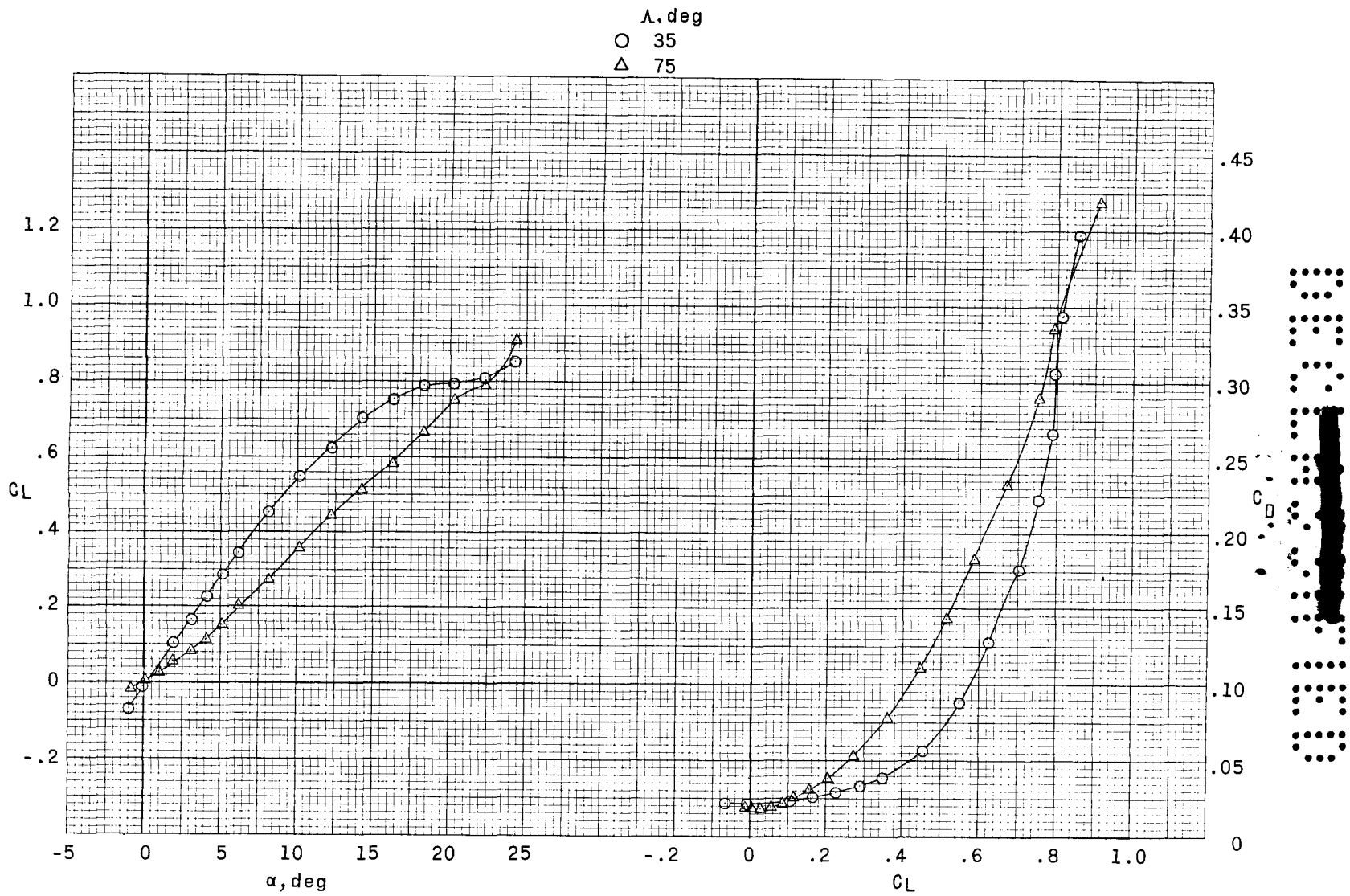

[redacted]

Figure 15.- Effect of wing leading-edge sweep angle on longitudinal aerodynamic characteristics of WFVHCE configuration with chord extension on main wing and horizontal tail set at $\Gamma_t = 10^{\circ}$. $\delta_c = 0^{\circ}$; $i_t = 0^{\circ}$.

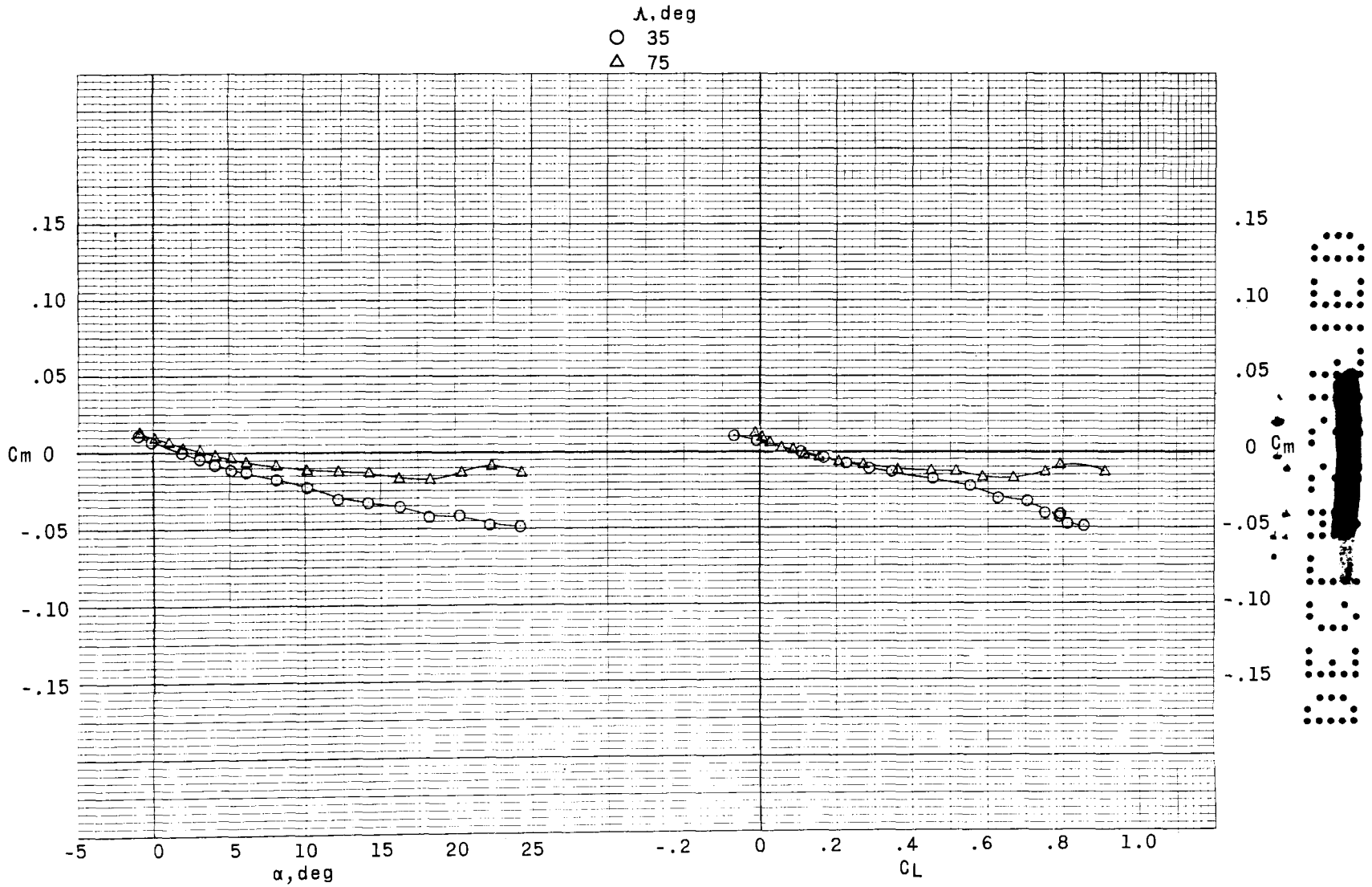

Figure 15.- Concluded.

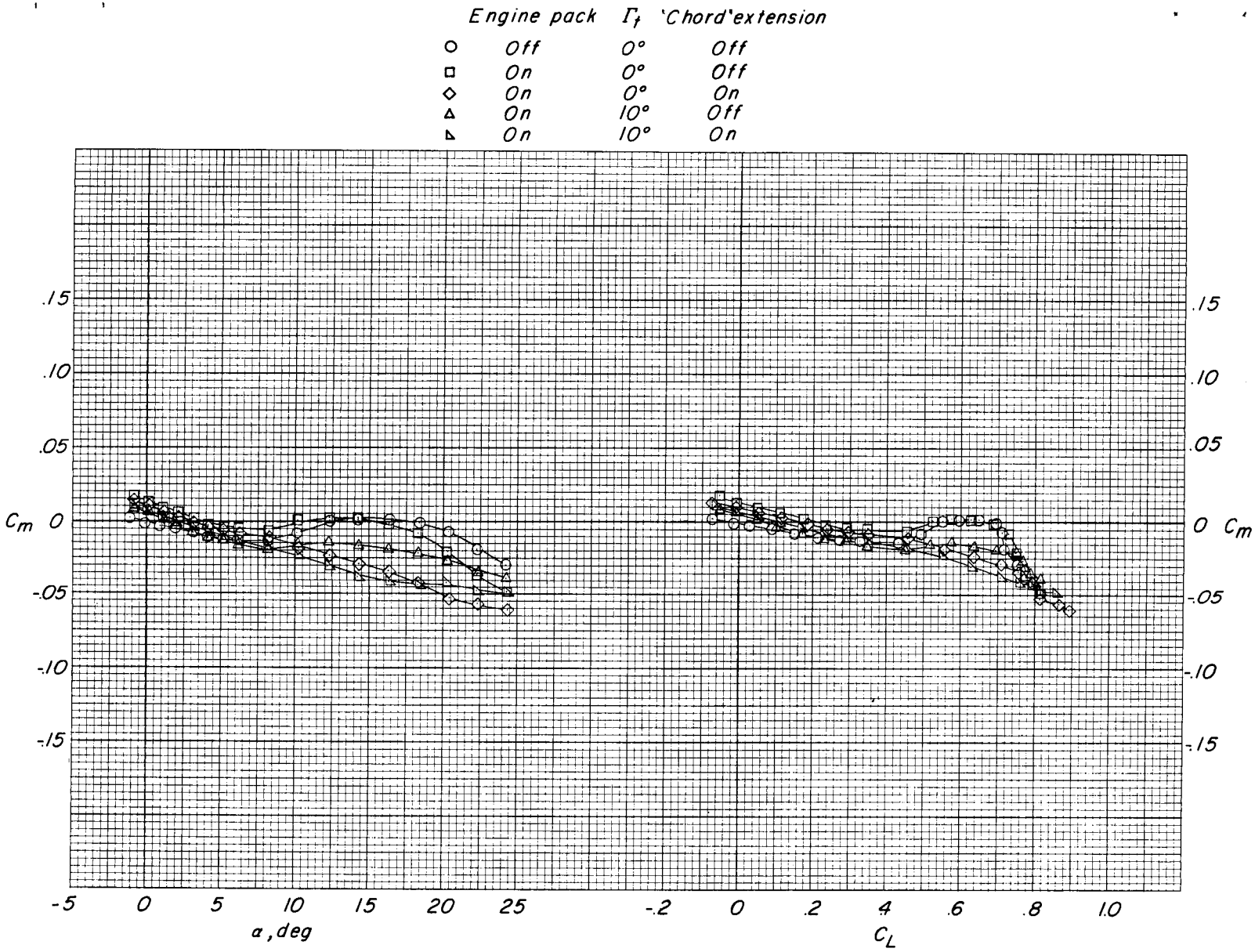

Figure 16.- Effect of engine pack, tail anhedral, and chord extension on pitching-moment characteristics of WFVHC configuration. $\Lambda = 35^{\circ}$; $\delta_c = 0^{\circ}$; $i_t = 0^{\circ}$.

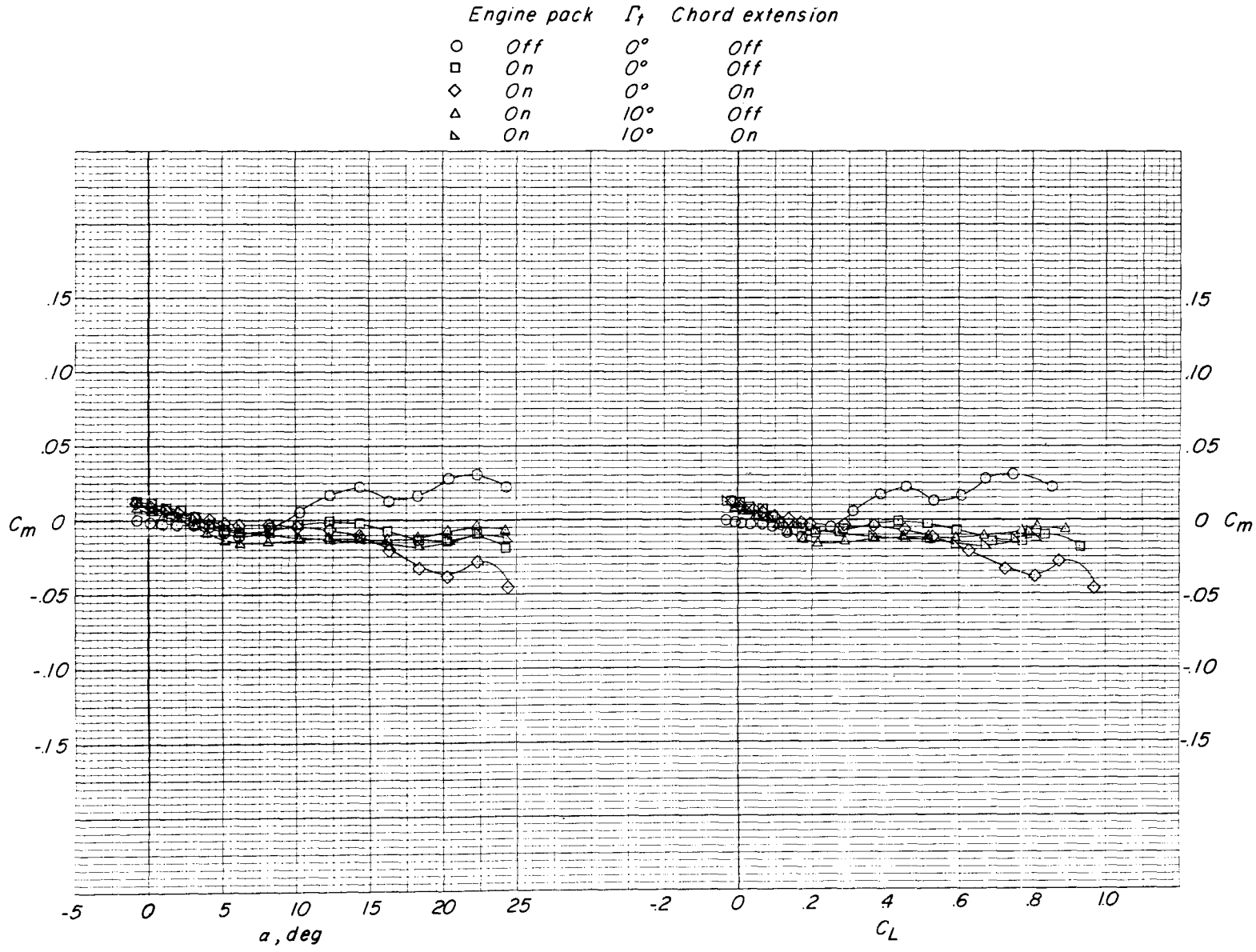

Figure 17.- Effect of engine pack, tail anhedral, and chord extension on pitching-moment characteristics of WFVHC configuration. $\Lambda = 75^{\circ}$; $\delta_c = 0^{\circ}$; $i_t = 0^{\circ}$.

[redacted]

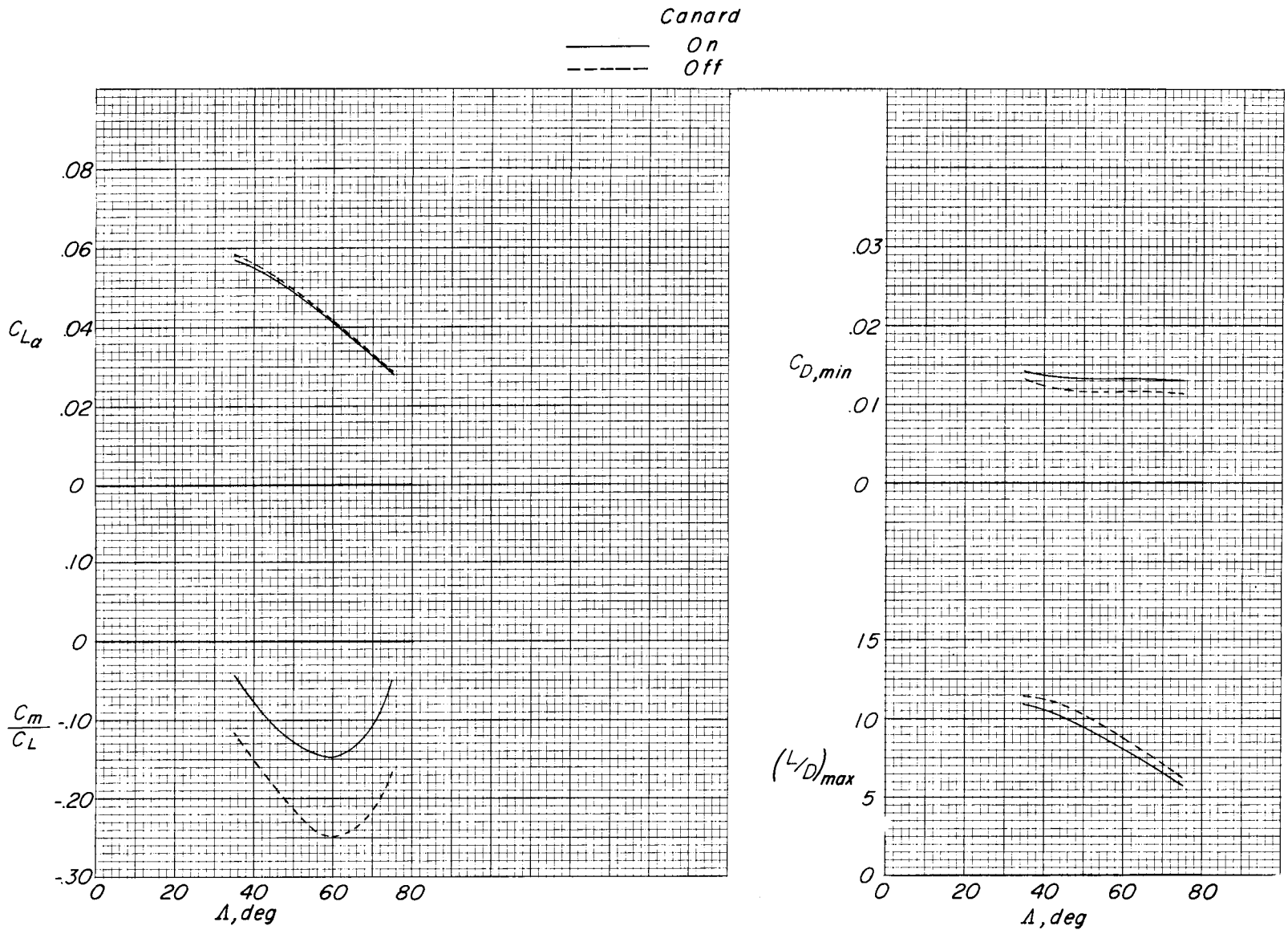

Figure 18.- Summary of longitudinal aerodynamic characteristics of WFVH configuration with and without canard. $i_t = 0^\circ$.

[redacted]

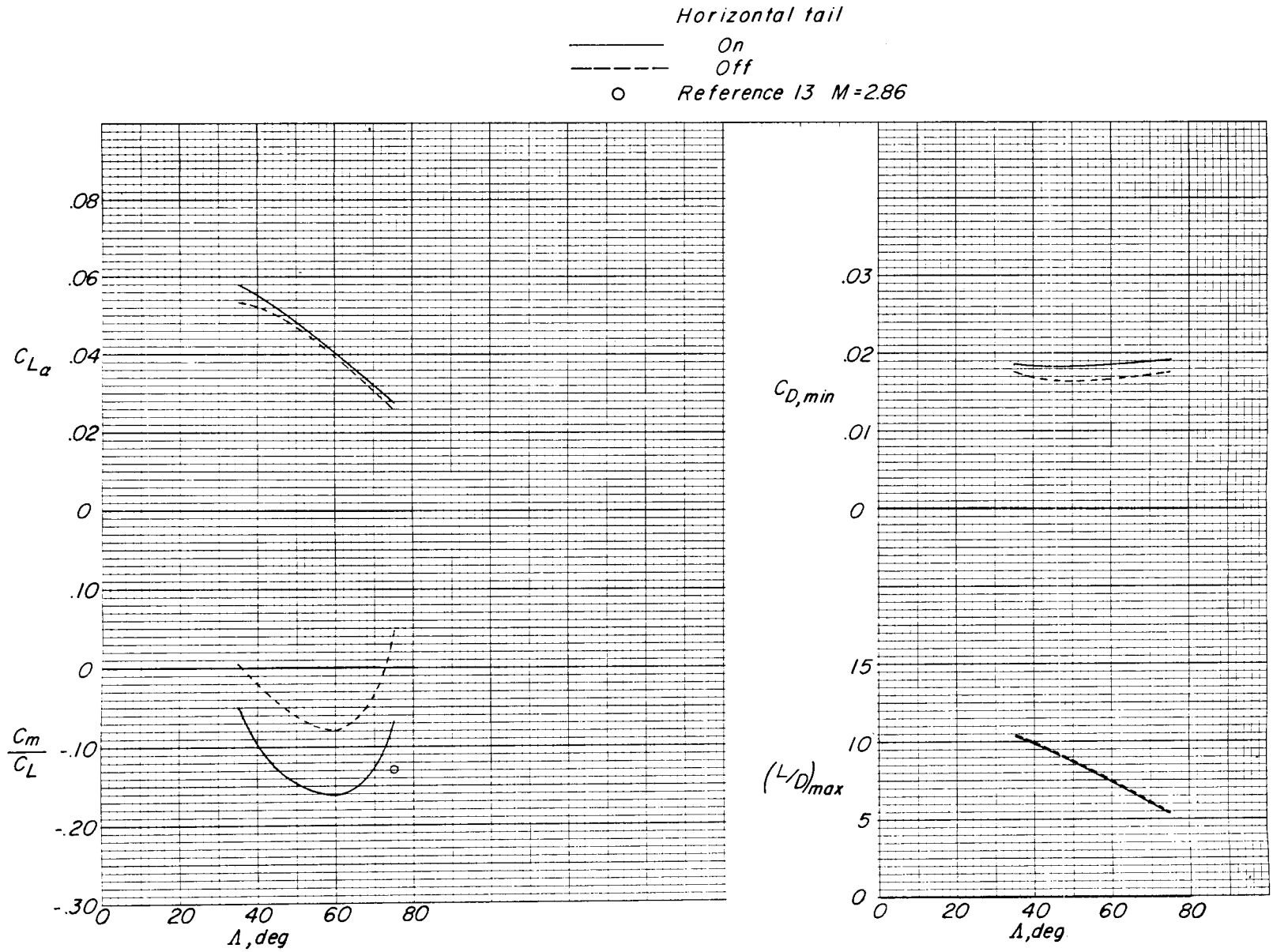

Figure 19.- Summary of longitudinal aerodynamic characteristics of WFVCE configuration with and without horizontal tail. $\delta_c = 0^\circ$.

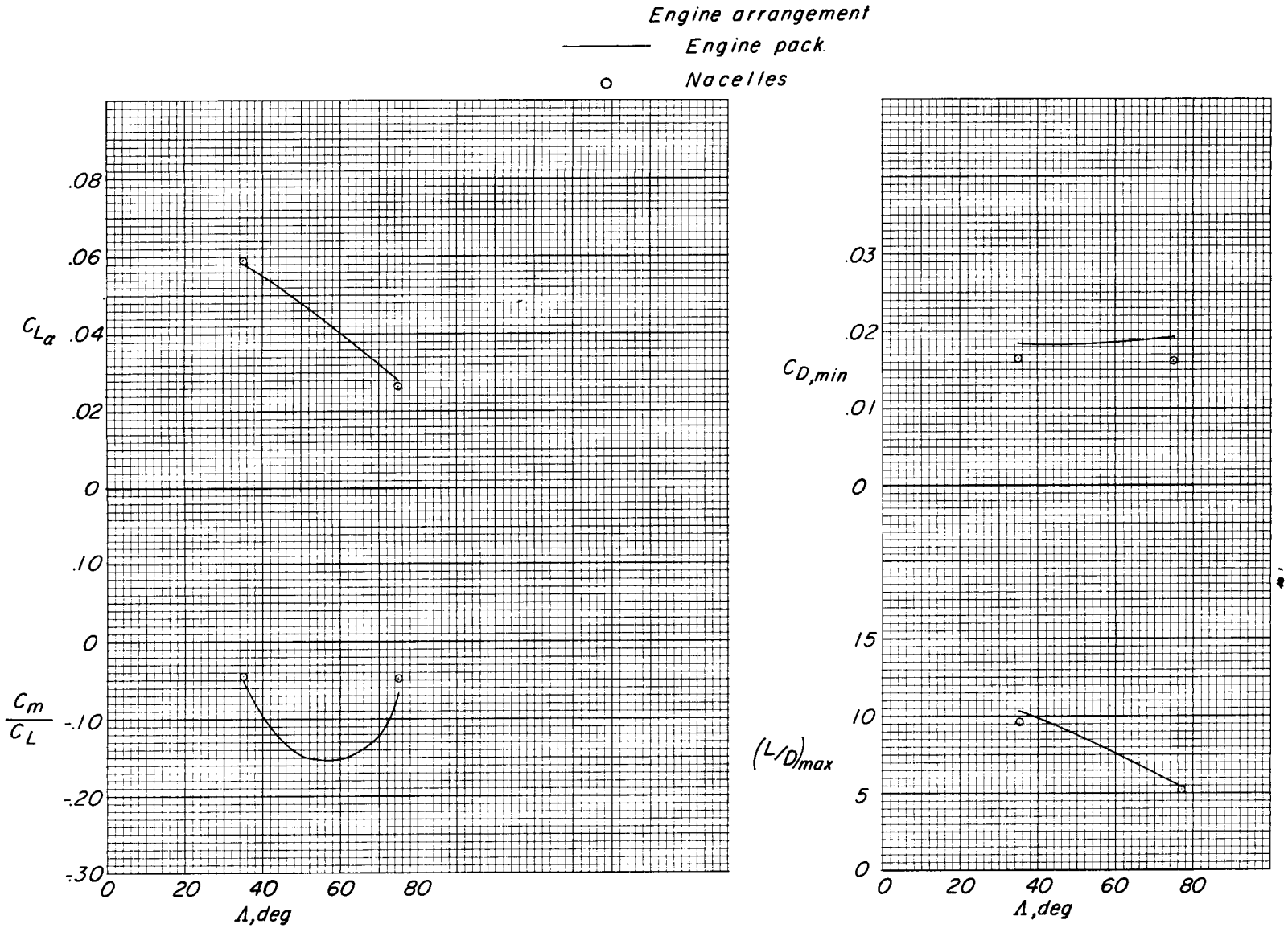

Figure 20.- Comparison of engine arrangements on longitudinal aerodynamic characteristics of WFVHC configuration. $\delta_c = 0^\circ$; $i_t = 0^\circ$.

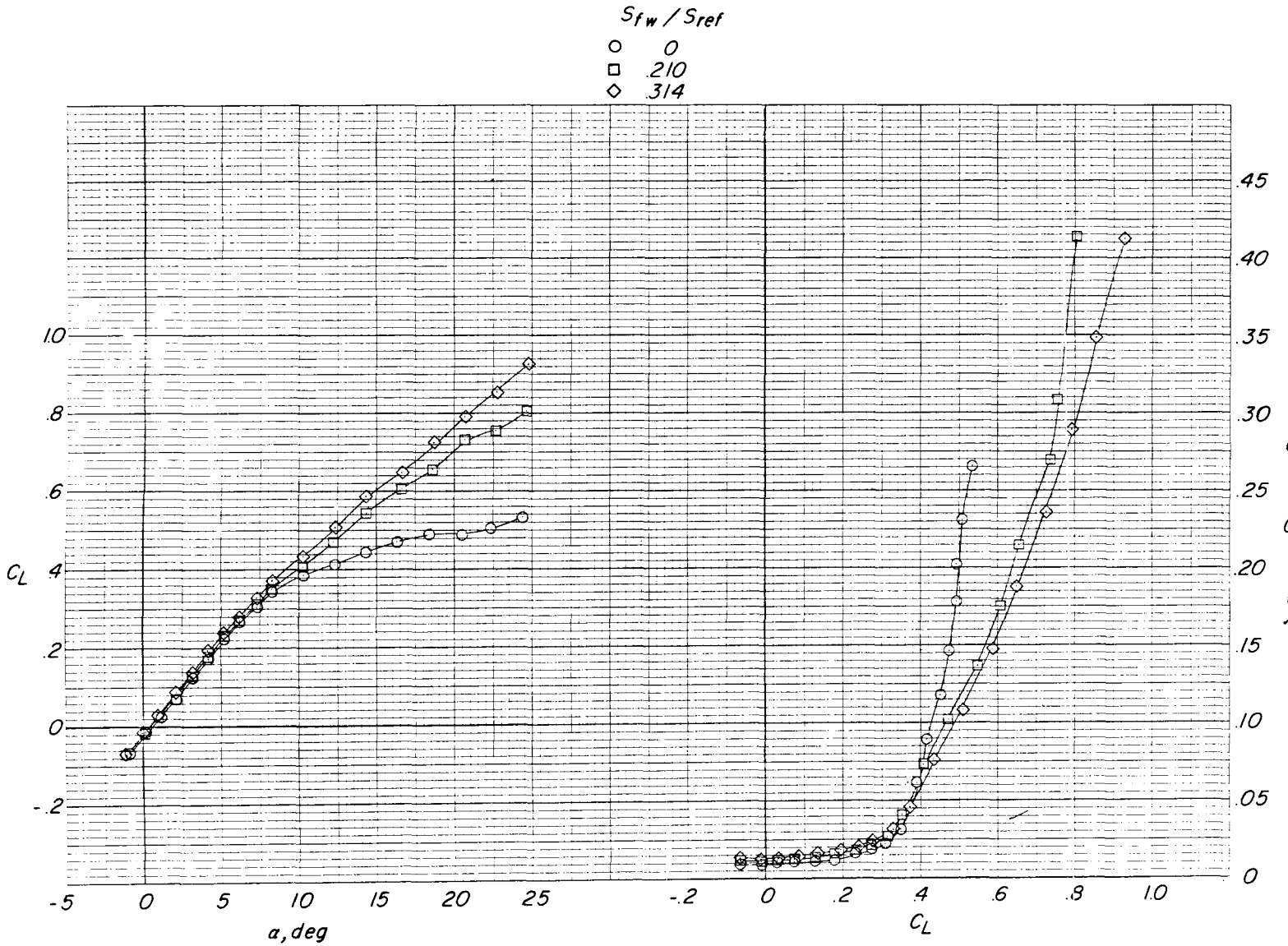

Figure 21.- Effect of addition of fore wings on longitudinal aerodynamic characteristics of WF configuration with 35° sweptback wing.

[redacted]

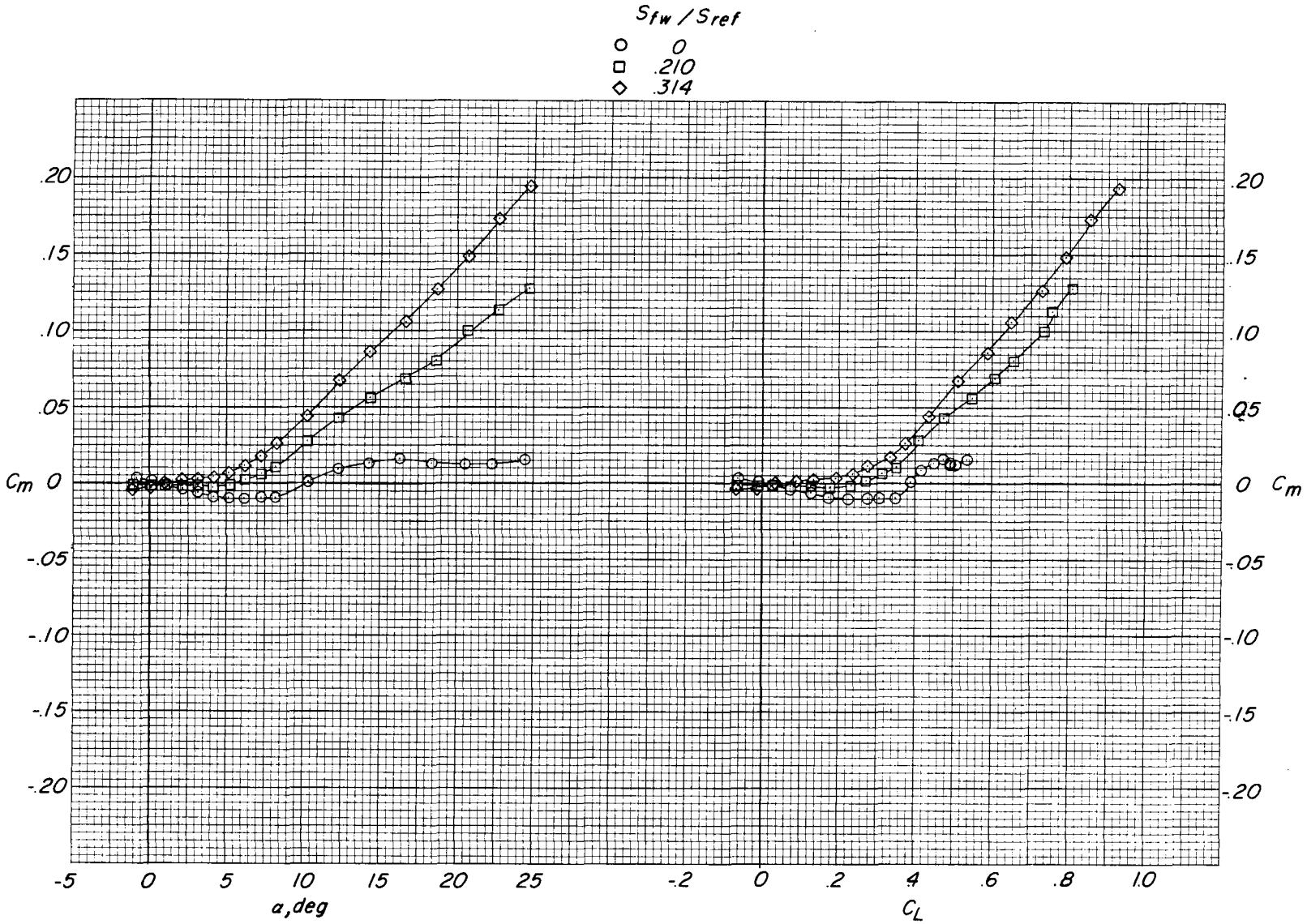

Figure 21.- Concluded.

[redacted]

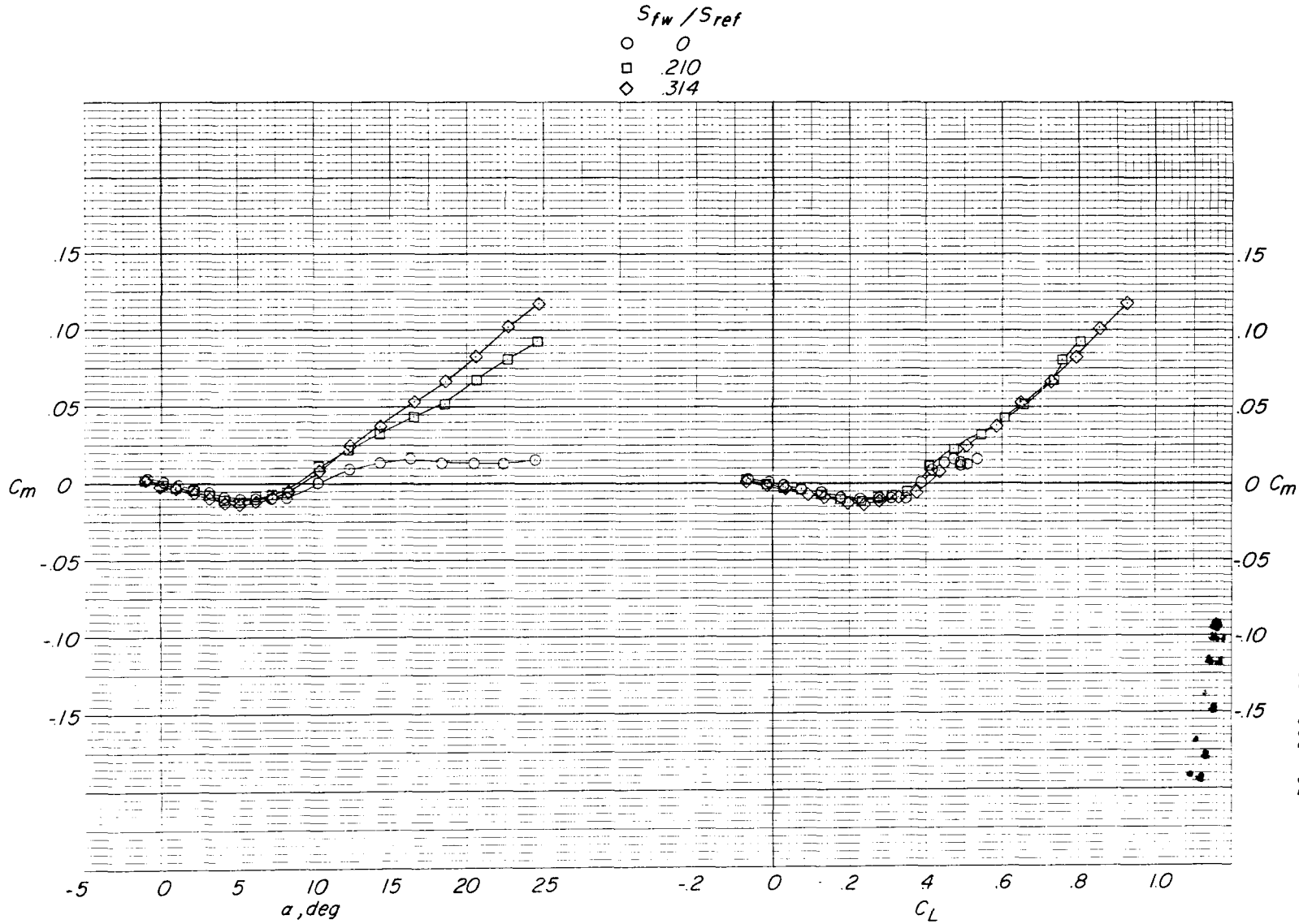

Figure 22.- Effect of addition of fore wings on pitching-moment characteristics of WF configuration with 35° sweptback wing. All configurations transferred to same stability level.

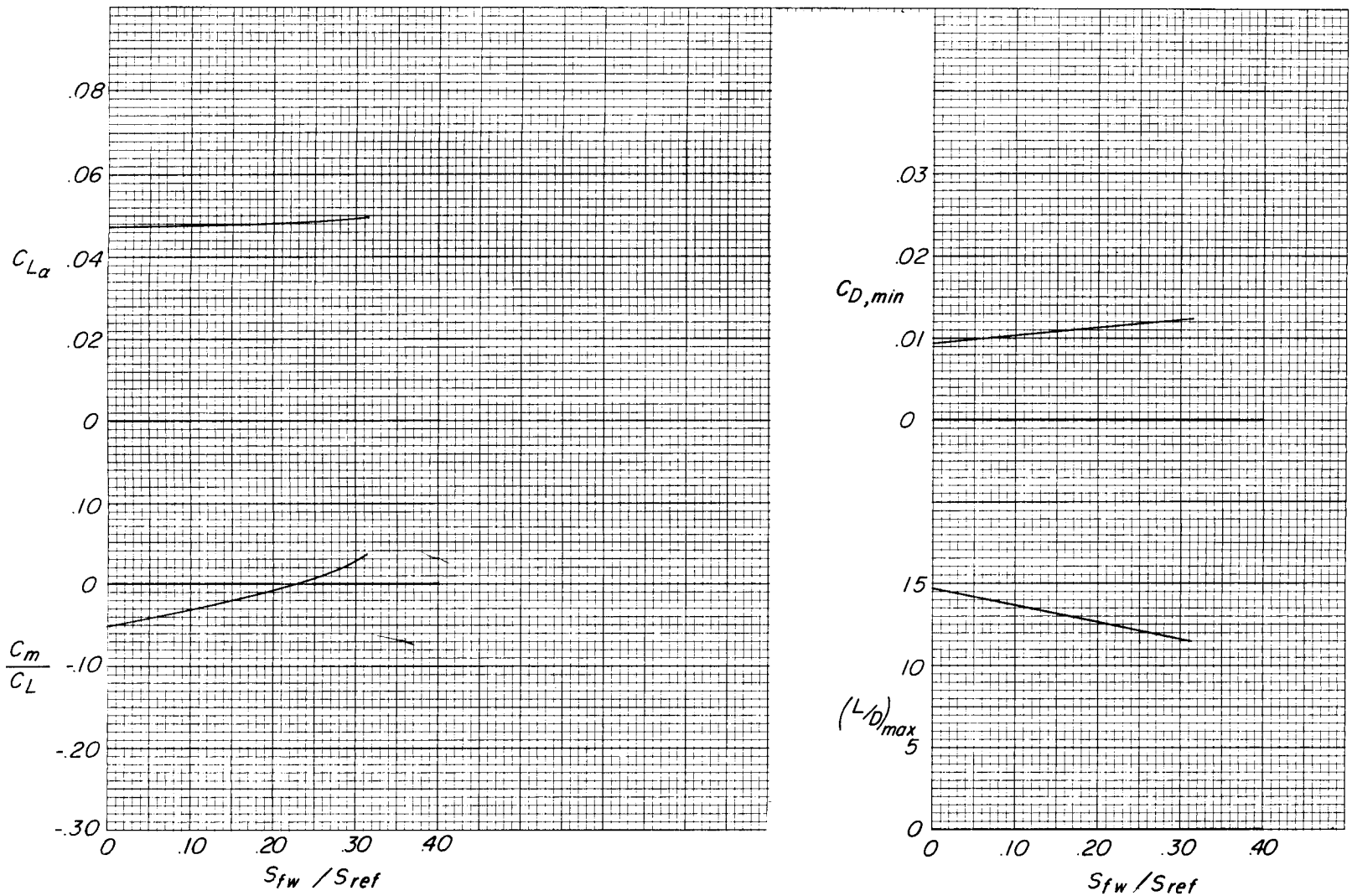

Figure 23.- Summary of effect of fore wings on longitudinal aerodynamic characteristics of WF configuration with 35° sweptback wing.

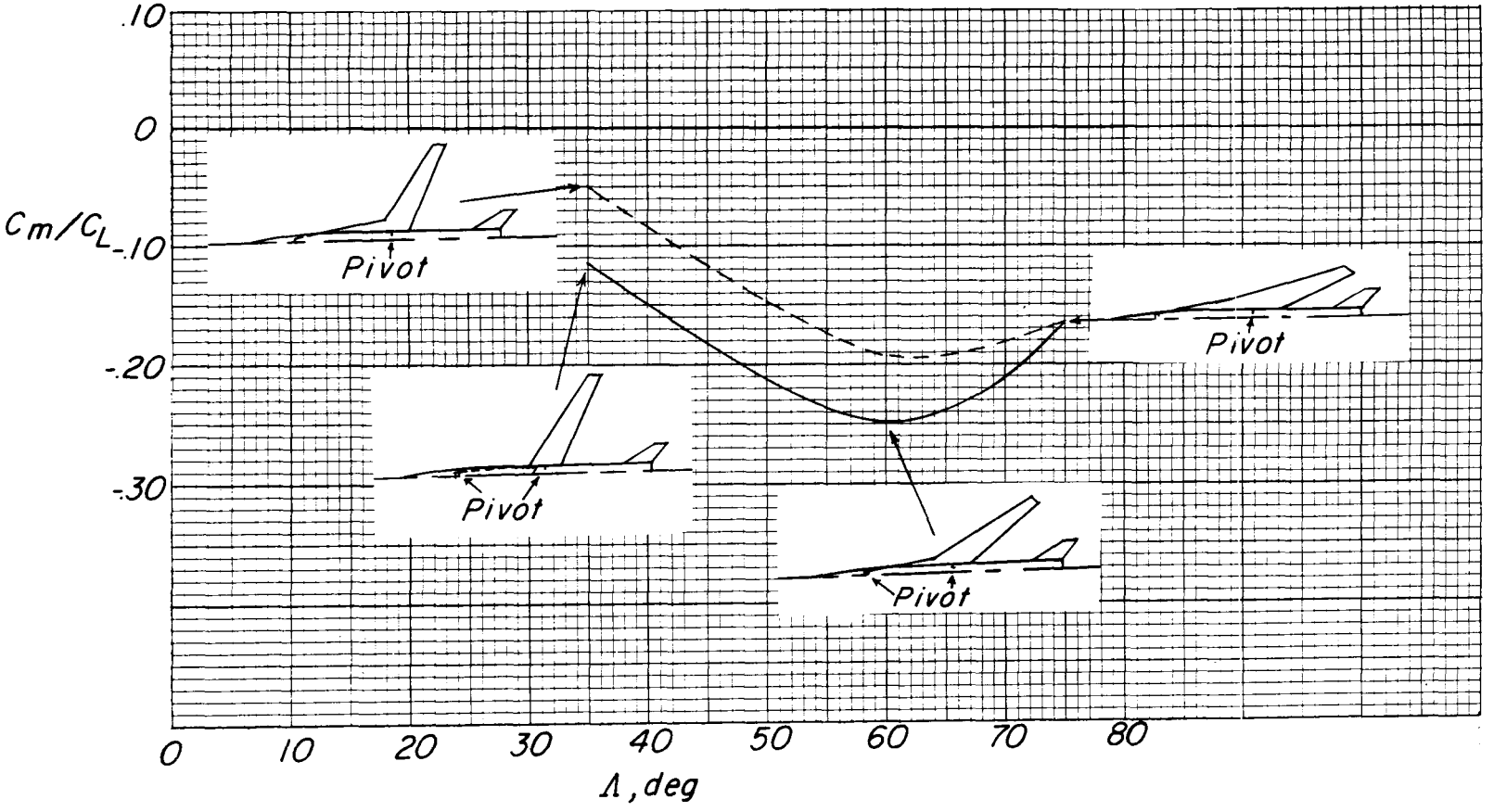

Figure 24.- Effect of fore wing on longitudinal-stability variation with wing sweep for WFVH configuration.